

Updated Constraints on the Minimal Supergravity Model

A. DJOUADI¹, M. DREES² and JEAN-LOIC KNEUR³

¹ *Laboratoire de Physique Théorique, UMR8627-CNRS,
Université Paris-Sud, Bt. 210, F-91405 Orsay, France.*

² *Dept. of Physics and Astronomy, University Of Hawaii, Honolulu, HI96822, USA*
and

Physikalisches Institut, Universität Bonn, Nussallee 12, 53115 Bonn, Germany¹.

³ *Laboratoire de Physique Théorique et Astroparticules, UMR5207-CNRS,
Université de Montpellier II, F-34095 Montpellier Cedex 5, France.*

Abstract

We provide an up-to-date analysis of the parameter space of the minimal supergravity model (mSUGRA). Novel features include the new central value of the top quark mass, an improved calculation of the masses of the supersymmetric particles and the neutral Higgs bosons, constraints from $b \rightarrow s\ell^+\ell^-$ decays, and a careful treatment of the most important experimental and theoretical uncertainties. In addition to the by now traditional plots of the allowed region in the $(m_0, m_{1/2})$ plane, we show allowed regions in the planes spanned by pairs of *physical* sparticle or Higgs boson masses. Moreover, we search for the minimal allowed masses of new particles for various sets of constraints. We find that in many cases the direct experimental limits from collider and Dark Matter searches can be saturated even in this minimal model, and even after including the by now quite restrictive constraint on the Dark Matter relic density.

¹Permanent address.

1. Introduction

The minimal supergravity model (mSUGRA) [1, 2] remains the most widely studied implementation of the minimal supersymmetric extension of the Standard Model (MSSM). It shares the virtues of a stable gauge hierarchy (for sparticle masses not much above a TeV) [3], possible Grand Unification of all gauge interactions [4], and a plausible Dark Matter (DM) candidate [5, 6] with all variants of the MSSM². Moreover, it manages to describe phenomenologically acceptable spectra with only four parameters plus a sign:

$$m_0, m_{1/2}, A_0, \tan\beta, \text{sign}\mu. \quad (1)$$

Here m_0 is the common soft supersymmetry breaking contribution to the masses of all scalars, $m_{1/2}$ the common supersymmetry breaking gaugino mass, and A_0 the common supersymmetry breaking trilinear scalar interaction (with the corresponding Yukawa coupling factored out); these three soft breaking parameters are taken at the scale M_X of Grand Unification, which we define as the scale where the properly normalized $SU(2)_L$ and $U(1)_Y$ gauge couplings meet. Finally, $\tan\beta$ is the ratio of the vacuum expectation values (vev's) of the two Higgs doublets at the weak scale, which we identify with the geometric mean of the soft breaking stop masses, and μ is the supersymmetric higgs(ino) mass parameter.

It should be admitted that the choice of parameters (1) is not particularly natural from a theoretical point of view: why should the scalar masses and trilinear A parameters all be exactly the same exactly at scale M_X ? From the perspective of supergravity theory, universality would seem to emerge more naturally at a scale closer to the (reduced) Planck mass, $M_P \simeq 2.4 \cdot 10^{18}$ GeV, if at all. However, while the possible unification of the gauge interactions makes a strong argument for a “grand desert” between the sparticle mass (or weak) and Grand Unified scales, physics at energy scales above M_X remains very speculative. At least as a first approximation it is therefore not unreasonable to impose our boundary conditions at scale M_X .

The ansatz (1) also has important virtues, in addition to its simplicity. It allows a quite varied phenomenology without violating any known constraints. In particular, the assumed flavor universality implies that supersymmetric flavor changing neutral current (FCNC) effects occur only radiatively, through renormalization group (RG) evolution. This keeps FCNC manageable, although, as we will see, flavor changing $b \rightarrow s\gamma$ and $b \rightarrow s\ell^+\ell^-$ decays do impose important constraints on the parameter space. A very appealing feature of mSUGRA is that it implements radiative breaking of the electroweak gauge symmetry [7], i.e. the RG evolution naturally drives the squared mass of one of the Higgs fields to negative

²A good DM candidate only emerges if R -parity is conserved, which we assume throughout.

values, keeping all squared sfermion masses positive. This allows to determine the absolute value of μ as function of the other parameters.

In spite of these successes, in recent years there has been a proliferation of analyses extending mSUGRA. Some of these extensions [8] are based on specific Grand Unified models, and thus have independent motivation from theory. However, in many phenomenological analyses universality between sfermion masses and/or the universality of soft breaking Higgs and sfermion masses is relaxed [9] without specific theoretical motivation³. Indeed, there seems to be a perception that the parameter space of the model is getting “squeezed” by ever tightening constraints.

Much of this perception probably comes from the by now quite accurate determination of the relic density of Dark Matter (DM) particles. At least in the framework of standard cosmology with a more or less scale invariant primordial spectrum of density perturbations, the analysis of large cosmological structures allows to infer the present DM density; the mapping of the microwave sky by WMAP plays an especially important role here [11]. This translates into a quite tight constraint on mSUGRA parameter space [12] under the standard assumption that all DM is formed by lightest superparticles (LSPs), which were in thermal equilibrium after the last period of entropy production⁴.

It should be emphasized that this tight constraint should not be cause for alarm. After all, the determination of the DM density, if taken at face value, constitutes a genuine signal of physics beyond the Standard Model (SM). Conceptually it should thus be considered on a par with, say, the measurement of a selectron mass. The fact that mSUGRA can accommodate this measurement is a further success of this model.

Nevertheless it seems timely to re-assess the mSUGRA model, taking recent theoretical and experimental developments into account. Besides the WMAP (and related) cosmological data, these include:

- More accurate calculations of leading two-loop corrections to the masses of neutral Higgs bosons [13], which makes it somewhat easier to satisfy the stringent Higgs search limits from LEP for a fixed value of the top quark mass;
- The new, somewhat lower central value of the mass of the top quark [14], which in turn goes in the direction of decreasing the predicted mass of the lightest neutral Higgs boson;

³Bucking this trend, there have also been a few recent studies where additional relations between the parameters in (1) are imposed [10].

⁴In standard cosmology this means the end of the inflationary epoch.

- Improved limits on radiative b decays and, in particular, first information on $b \rightarrow s\ell^+\ell^-$ decays, which excludes scenarios where the sign of the amplitude of $b \rightarrow s\gamma$ decays is opposite to the SM prediction [15];
- A growing (though not global) consensus [16] that the SM prediction for hadronic contributions to the anomalous dipole moment of the muon based on data from e^+e^- colliders is more reliable, which again elevates the discrepancy between the measurement [17] of $a_\mu - 2$ and its SM prediction [18] to the level of ~ 2.5 standard deviations.

Several analyses of this kind have appeared in the last few years [12], whose results broadly agree with our's if we take the old value of the top mass, $m_t = 178$ GeV. The effect of the new, reduced (central) value of m_t has so far only been analyzed in refs. [19, 20]; these papers have little overlap with our's. Usually the results of mSUGRA parameter scans are presented as allowed regions in the $(m_0, m_{1/2})$ plane. We also present similar allowed regions in the planes spanned by *physical* sparticle or Higgs boson masses; this should give a more direct overview of the kind of spectra that can be generated in mSUGRA. To the best of our knowledge, similar results have previously only been published in the (by now quite dated) review article [21].

Moreover, we put special emphasis on a careful treatment of theoretical and experimental uncertainties. This allows us to derive conservative lower bounds on the masses of superparticles and Higgs bosons in mSUGRA, for different sets of assumptions. We find that in many cases the direct experimental search limits can be saturated even if all relevant constraints are taken at face value. The main exceptions are the masses of the gluino and of first and second generation squarks, which are forced by the assumption of gaugino mass unification to lie at least 100 to 150 GeV above the current Tevatron limits. Imposing the DM constraint does *not* affect these lower bounds very much.

The remainder of this article is organized as follows. In the next chapter we briefly describe calculational details and the constraints we impose. Sec. 3 updates ref. [22] by showing the allowed regions in the $(m_0, m_{1/2})$ plane, as well as in the planes spanned by pairs of physical masses, for a few values of $\tan\beta$. Sec. 4 is devoted to a discussion of minimal masses of sparticles and Higgs bosons that are compatible with various sets of constraints. Finally, in Sec. 5 we summarize our main results and draw some conclusions.

2. Scanning Procedures

We use the FORTRAN program SuSpect [23] to calculate the spectrum of superparticles and Higgs bosons. Since these masses are defined at the weak scale while the dimensionful input

parameters in (1) are defined at the scale of Grand Unification, the program has to integrate the set of coupled renormalization group equations connecting these two scales; SuSpect now uses two-loop equations [24] for all relevant quantities (gauge and Yukawa couplings, μ , and the soft breaking parameters). The program also computes the one-loop and dominant two-loop corrections to the Higgs potential, as well as the dominant one-loop corrections turning the running ($\overline{\text{DR}}$) quark, lepton and sparticle masses into on-shell (pole) masses. The calculation of the neutral Higgs boson masses includes leading two-loop corrections [13]. See ref. [23] for further details on the calculation of the spectrum.

Not all combinations of input parameters lead to radiative $SU(2)_L \times U(1)_Y \rightarrow U(1)_{\text{QED}}$ symmetry breaking. This imposes a first constraint on the parameter space. We also exclude parameter sets where the scalar potential has deep minima breaking charge and/or color *at the weak scale* [25]. As usual in the literature [12], we do not veto scenarios where the absolute minimum of the scalar potential occurs for field values intermediate between the weak and GUT scales [26], since the tunneling rate into these minima is exceedingly slow. In the language of ref. [26], we impose the ‘‘CCB’’ constraints, which exclude very large values of $|A_0|/\sqrt{m_0^2 + m_{1/2}^2}$, but do not impose the ‘‘UFB’’ constraints.

We next impose experimental constraints. To begin with, the strong upper limits on the abundance of stable charged particles [27] exclude scenarios where the lightest superparticle is charged. This excludes cases with $m_0 \ll m_{1/2}$ where $\tilde{\tau}_1$ tends to be the LSP (especially at large $\tan\beta$), and some combinations with $m_0 \gtrsim m_{1/2}$ and sizable $|A_0|$, where \tilde{t}_1 is the LSP⁵.

We also impose the lower bounds on sparticle and Higgs masses that result from collider searches. We interpret the LEP limits from searches for (unstable) charged superparticles as requiring

$$\sigma(e^+e^- \rightarrow \tilde{X}\tilde{X}^*; \sqrt{s} = 209 \text{ GeV}) < 20 \text{ fb} \quad (2)$$

separately for each relevant mode ($\tilde{X} = \tilde{t}_1, \tilde{\tau}_1, \tilde{\chi}_1^+$). This effectively imposes lower bounds of 104.5 GeV on the mass of the lighter chargino $\tilde{\chi}_1^+$, 101.5 GeV for the lighter scalar top eigenstate \tilde{t}_1 , and 98.8 GeV for the lighter scalar τ eigenstate $\tilde{\tau}_1$. For non-pathological situations these agree closely with the limits published by the LEP experiments [27, 30].⁶

The limits from the searches for Higgs bosons at LEP also impose important constraints on the parameter space. Of special importance is the limit on $e^+e^- \rightarrow ZH$ with $H \rightarrow b\bar{b}$.

⁵These constraints can be evaded if the LSP resides in the hidden sector (e.g., if it is the gravitino [28]), or in extensions of mSUGRA where the LSP is an axino [29].

⁶The only ‘‘pathological’’ situation that can be relevant in mSUGRA is the case of small $\tilde{\tau}_1 - \tilde{\chi}_1^0$ mass splitting. However, at small $\tan\beta$ selectron searches at LEP will lead to constraints on the parameter space that are nearly as strong as those from $\tilde{\tau}_1$ searches. At high $\tan\beta$, scenarios with small slepton and neutralino masses are excluded by the g_μ constraint.

In the SM it leads to the bound [31] $m_H^{\text{SM}} > 114$ GeV. For small and intermediate values of $\tan\beta$ this bound applies directly to the light scalar Higgs boson in mSUGRA, but for $\tan\beta \gtrsim 50$ its coupling to the Z boson can be suppressed significantly. We parameterize this dependence as in ref. [22], except that the constant (coupling-independent) term is increased by 0.5 GeV in order to reflect the increase of the limit that resulted from combining the limits from the four LEP experiments.

We also include constraints from quantum corrections due to superparticles. These include the upper bound

$$\delta\rho_{\text{SUSY}} < 2.2 \cdot 10^{-3} \quad (3)$$

on the supersymmetric contribution to the electroweak ρ -parameter [32], including 2-loop QCD corrections [33]. However, it turns out that this constraint is always superseded by either the LEP Higgs search limit or by the CCB constraint.

A more significant constraint arises from the precise measurements of the anomalous magnetic moments of positively and negatively charged muons [17]. As well known by now, the interpretation of this measurement hinges on whether data from semileptonic τ decays are used for the evaluation of the SM prediction or if one only relies on data from e^+e^- annihilation into hadronic final states. In the former case the measurement agrees quite well with the SM, whereas in the latter case the prediction falls $\sim 2.5\sigma$ short of the measurement [18]. In order to reflect this uncertainty, we impose either the more conservative constraint

$$-5.7 \cdot 10^{-10} \leq a_{\mu, \text{SUSY}} \leq 4.7 \cdot 10^{-9}, \quad (4)$$

which describes the overlap of the 2σ limits derived from the two competing SM predictions, or the more aggressive constraint

$$1.06 \cdot 10^{-9} \leq a_{\mu, \text{SUSY}} \leq 4.36 \cdot 10^{-9}, \quad (5)$$

which is the 90% c.l. range derived using the e^+e^- data only. Here $a_{\mu, \text{SUSY}}$ is the sparticle loop contribution to $a_\mu \equiv (g_\mu - 2)/2$. The SM prediction based on e^+e^- data is nowadays considered to be more reliable [16]. Note that (4) allows the supersymmetric contribution to vanish, or even be slightly negative, whereas (5) requires it to be positive. Our calculation of $a_{\mu, \text{SUSY}}$ is based on ref. [34], modified to include leading logarithmic QED 2-loop corrections [35] which increase $a_{\mu, \text{SUSY}}$ by $\sim 5\%$.

The constraints discussed so far are all quite robust against minor changes of the model. In particular, deviating from exact universality of scalar masses or, equivalently, allowing small flavor non-diagonal entries of the sfermion mass matrices, will not change any of these

bounds significantly. This is quite different for the bounds from inclusive $b \rightarrow s\gamma$ decays, which are also widely included in analyses of the parameter space of mSUGRA and similar models [8, 9, 10, 12]. Including theoretical uncertainties of the SM prediction [36] as well as the experimental measurement [27] (now statistically dominated by BELLE data), we require the calculated branching ratio to fall in the range

$$2.65 \cdot 10^{-4} \leq B(b \rightarrow s\gamma) \leq 4.45 \cdot 10^{-4}. \quad (6)$$

Our calculation of this branching ratio is based on ref. [37], which – for heavy sparticles – includes the dominant QCD corrections to the $\tilde{\chi}^{\pm}\tilde{t}$ loop corrections, which (together with tH^{\pm} loops) dominate the supersymmetric contributions in all supersymmetric models where flavor violation is assumed to be described entirely by the Kobayashi–Maskawa (KM) matrix. For large $\tan\beta$ and not too heavy sparticles these contributions can be quite large; for $\mu > 0$ they can even flip the sign of the amplitude relative to the SM prediction, leading to a second allowed region [22] when the modulus of this amplitude approaches its SM value. However, it has recently been argued [15] that new data on $b \rightarrow s\ell^+\ell^-$ data strongly disfavor this possibility, since such a flip of sign would change the interference between penguin diagrams (similar to those contributing to $b \rightarrow s\gamma$) and (new) box diagrams. We therefore impose the additional constraint that the amplitude for $b \rightarrow s\gamma$ decays should have the sign predicted in the SM.

The range (6) should perhaps be extended somewhat, since the MSSM prediction has larger theoretical uncertainties than that in the SM. To begin with, ref. [37] includes NLO QCD corrections to the supersymmetric contribution only in the limit of heavy sparticles, as remarked above. Note also that the determination of the KM element V_{ts} , to which all contributions to the amplitude describing $b \rightarrow s\gamma$ decays are proportional, can be affected by supersymmetric contributions to processes in the K sector, which in the SM lead to tight constraints on this quantity. More importantly, the constraint imposed by (6) on the parameters listed in (1) will evaporate entirely if a modest amount of $\tilde{b} - \tilde{s}$ mixing is allowed at the GUT scale [38]. This would lead to one-loop gluino-mediated box diagram contributions to $b \rightarrow s\gamma$ decays [39]. Since for strict scalar universality all contributions are suppressed by a factor $|V_{ts}| \simeq 0.04$, even a small amount of $\tilde{b} - \tilde{s}$ mixing would lead to new contributions of comparable size. The sign of this new contribution is given by the sign of the corresponding mixing angle, which is a free parameter in this slightly extended model. At the price of modest fine-tuning one could thus make any set of mSUGRA parameters “ $b \rightarrow s\gamma$ compatible”. Since the required squark flavor mixing would still be quite small, it would have negligible effects on (flavor conserving) signals at colliders, radiative corrections to the MSSM Higgs sector, etc. The constraint (6) thus has a different status from the

constraints discussed earlier. In Sec. 4 we will therefore present limits on sparticle and Higgs boson masses with or without this additional constraint.

The last, and very restrictive, constraint that is usually imposed in analyses of constrained supersymmetric models is based on the determination of the density of non-baryonic Dark Matter (DM) from detailed analyses of the anisotropies of the cosmic microwave background (CMB), in particular by the WMAP experiment [11]. At 99% c.l., they find

$$0.087 \leq \Omega_{\text{DM}} h^2 \leq 0.138. \quad (7)$$

Here Ω measures the mass (or energy) density in units of the critical density, whereas h is the scaled Hubble constant. The emergence of the cosmological “concordance model” is undoubtedly a great triumph of modern cosmology. One should nevertheless be aware that the result (7) is based on several assumptions, which are reasonable but not easy to cross-check independently [40]. In particular, one has to assume that simple inflationary models give essentially the right spectrum of primordial density perturbations. Without this, or a similarly restrictive, ansatz for this spectrum, the result (7) would evaporate. In the absence of a generally accepted estimate of the theoretical uncertainty from the assumed ansatz of the primordial density perturbations, we decided to take the 99% c.l. region of the DM relic density, as opposed to the 90% or 95% c.l. regions used for quantities measured in the laboratory.

In order to translate the constraint (7) into a constraint on mSUGRA parameters, one has to make several *additional* assumptions. The lightest neutralino $\tilde{\chi}_1^0$ must be essentially stable, which, in the context of mSUGRA with conserved R -parity, requires it to be heavier than the gravitino [28]. In addition, one must assume that standard cosmology (with known Hubble expansion rate, and no epoch of entropy production) can be extrapolated backwards to temperatures of at least $\sim 5\%$ of $m_{\tilde{\chi}_1^0}$. In that case $\tilde{\chi}_1^0$ was in full thermal equilibrium with the SM plasma, making today’s $\tilde{\chi}_1^0$ density independent of the “re-heat” temperature of the Universe T_R at the end of inflation. With these assumptions, our calculation of the relic density proceeds as in ref. [22]. Without these assumptions, no meaningful constraint on the parameters (1) results. In Sec. 4 we therefore again present results with or without the constraint (7).

3. Results of the scans

3.1 $(m_0, m_{1/2})$ parameter space

Examples of scans of the $(m_0, m_{1/2})$ plane are shown in Figs. 1 through 6. Figs. 1 and 2 represent our “base choice”, $m_t = 172.7$ GeV (the current central value [14]), $A_0 = 0$ and

$\mu > 0$. The light grey regions are excluded by theoretical constraints (in particular, by the requirement of correct electroweak symmetry breaking), as well as by the searches for sparticles, i.e. by the constraint (2). The dark grey areas are excluded by the requirement that the LSP be neutral, in particular by $m_{\tilde{\tau}_1} > m_{\tilde{\chi}_1^0}$. The pink regions are excluded by searches for neutral Higgs bosons at LEP. The light pink regions are excluded even if we allow for a 3 GeV theoretical uncertainty in the calculation of m_h in the MSSM, i.e. if we only exclude (SM-like) Higgs bosons with calculated mass $m_h \leq 111$ GeV. In the medium pink region the predicted m_h lies between 111 and 114 GeV, which might be acceptable if unknown higher order corrections are sufficiently large and positive. As well known, the LEP data [31] show some (weak) evidence for the existence of an SM-like Higgs boson with mass near 114 GeV; the mSUGRA regions that can explain this small excess of Higgs-like events are shown in red.

In the blue regions the SUSY contribution to the anomalous magnetic moment of the muon falls in the range (5) favored by e^+e^- data; recall that in this case a positive SUSY contribution is required at the $\sim 2.5\sigma$ level. The green region is excluded by the constraint (6) on the branching ratio for radiative $b \rightarrow s\gamma$ decays. Finally, in the black regions the $\tilde{\chi}_1^0$ relic density lies in the desired range (7).

We see that the Higgs search limits are very severe for small and moderate values of $\tan\beta$, and/or for smaller values of m_t ; for example, for $m_t = 172.7$ GeV, $\tan\beta = 5$ and $A_0 = 0$ (Fig. 2) they imply $m_{1/2} \gtrsim 0.6$ TeV for small m_0 , or $m_0 \gtrsim 2$ TeV for small $m_{1/2}$. At first the region excluded by this constraint shrinks quickly with increasing $\tan\beta$, but it becomes almost independent of this parameter once $\tan\beta \gtrsim 20$. These regions become even larger if m_t is below its current central value. For example, Fig. 3 shows that the region excluded by this constraint for $\tan\beta = 10$ and $m_t = 166.9$ GeV, the current 95% c.l. lower bound on this quantity, is very similar to that for $\tan\beta = 5$ and m_t at its current central value. Conversely, again for $\tan\beta = 10$, increasing m_t to the previous central value of 178 GeV [41] (which happens to be quite close to the current 95% c.l. upper bound) reduces the lower bound on $m_{1/2}$ for small m_0 to about 250 GeV, and allows values of m_0 down to about 750 GeV even if $m_{1/2}$ is small, see Fig. 4. All these numbers allow for a 3 GeV theoretical uncertainty in m_h .

The (green) regions excluded by the $b \rightarrow s\gamma$ constraints shows the opposite dependence on $\tan\beta$, becoming larger as this parameter increases. Note, however, that for $m_t = 172.7$ GeV and $A_0 = 0$ (Figs. 1 and 2) the Higgs constraint supersedes the $b \rightarrow s\gamma$ constraint for values of $\tan\beta$ up to $\tan\beta = 50$, unless one assumes that unknown higher-order corrections to m_h are large and positive. For the highest value displayed, $\tan\beta = 58$, the $b \rightarrow s\gamma$

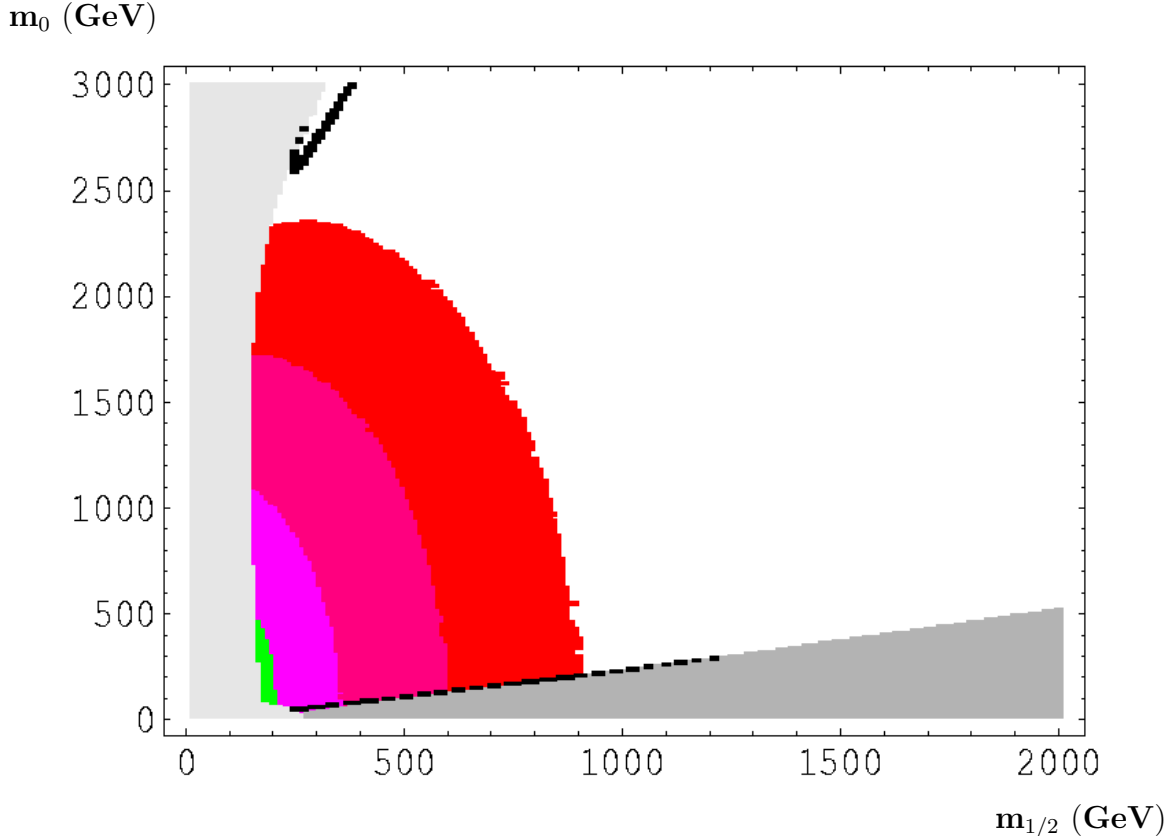


Figure 1: *The $mSUGRA$ $(m_{1/2}, m_0)$ parameter space with all constraints imposed for $A_0 = 0, \mu > 0$ and $\tan\beta = 10$. The top quark mass is fixed to the new central value, $m_t = 172.7$ GeV. The light grey region is excluded by the requirement of correct electroweak symmetry breaking, or by sparticle search limits. In the dark grey region $\tilde{\tau}_1$ would be the LSP. The light pink region is excluded by searches for neutral Higgs bosons at LEP, whereas the green region is excluded by the $b \rightarrow s\gamma$ constraint (6). In the blue region, the SUSY contribution to $g_\mu - 2$ falls in the range (5), whereas the red regions are compatible with having an SM-like Higgs boson near 115 GeV. Finally, the black regions satisfy the DM constraint (7).*

constraint excludes an additional domain close to the region where electroweak symmetry breaking does not take place; in this area, the charged Higgs boson is relatively light and the tH^\pm contribution (which is not compensated by the $\tilde{t}\tilde{\chi}^\pm$ ones, as the top squarks are rather heavy) leads to a value of $B(b \rightarrow s\gamma)$ that is slightly higher than the upper bound $B_{\max} = 4.45 \cdot 10^{-4}$.

Figs. 3 and 4 show that reducing (increasing) m_t further reduces (increases) the importance of the $b \rightarrow s\gamma$ constraint relative to the Higgs search constraint. Taking sizable (negative) values of A_0 also increases the relative importance of the $b \rightarrow s\gamma$ constraint, as shown by Figs. 5 and 6.⁷

⁷The effects of $A_0 \neq 0$ have recently been studied in [42].

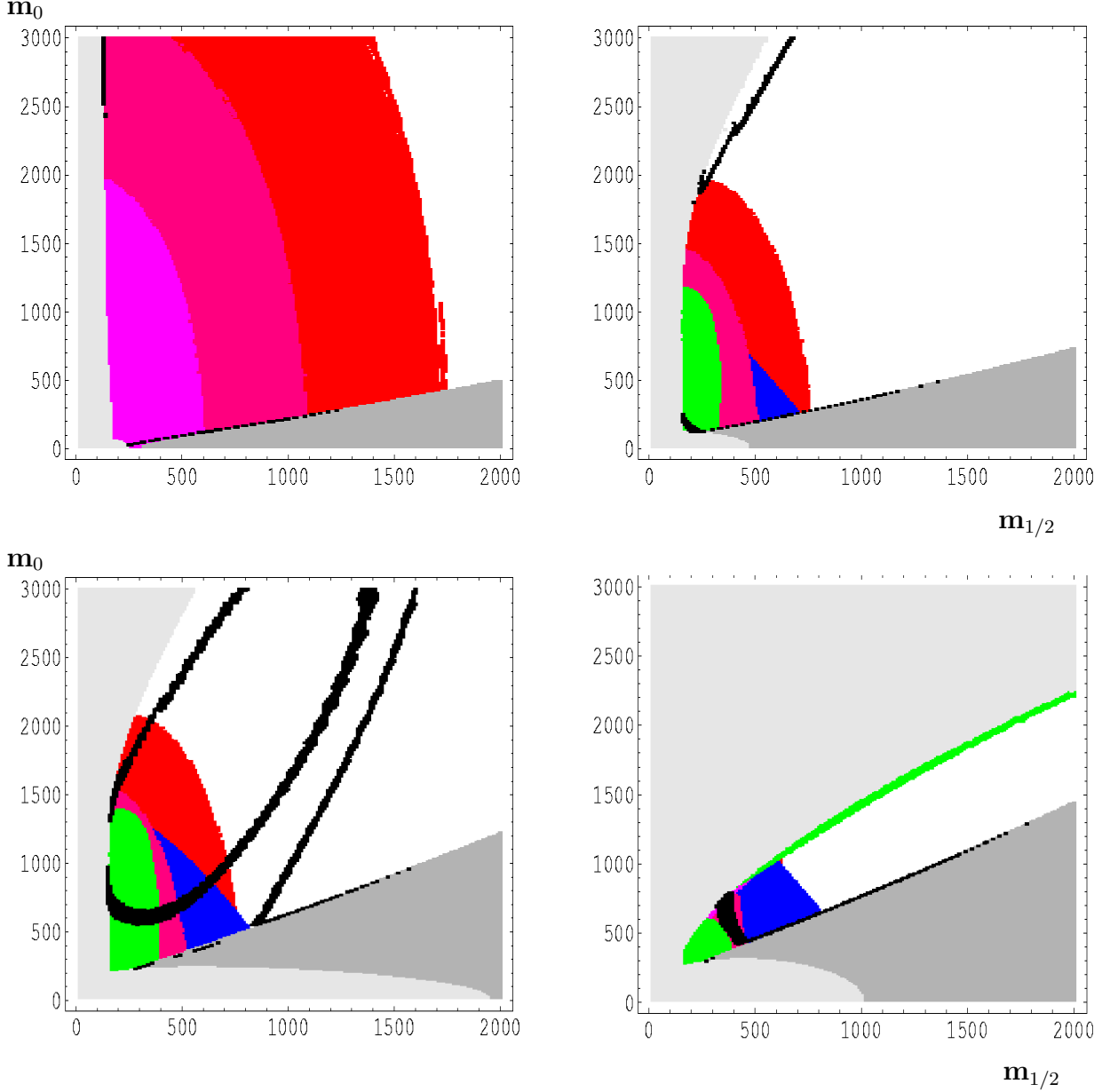


Figure 2: The $mSUGRA$ $(m_{1/2}, m_0)$ parameter space with all constraints imposed for $A_0 = 0, \mu > 0$ and the values $\tan \beta = 5$ (top left), 30 (top right), 50 (bottom left) and 58 (bottom right). The top quark mass is fixed to the new central value, $m_t = 172.7$ GeV. Notation and conventions are as in Fig. 1.

For example, for $\tan \beta = 30$ and $A_0 = -2$ TeV (Fig. 6) the region excluded by the $b \rightarrow s\gamma$ constraint even excludes some combinations of parameters with predicted m_h well above 115 GeV. The predicted branching ratio for $b \rightarrow s\gamma$ decays is quite sensitive to A_0 since the main supersymmetric contribution comes from stop–chargino loops, and stop mixing is affected quite strongly by A_0 , as long as $|A_0| \gtrsim m_{1/2}$. Recall, however, that this constraint can be

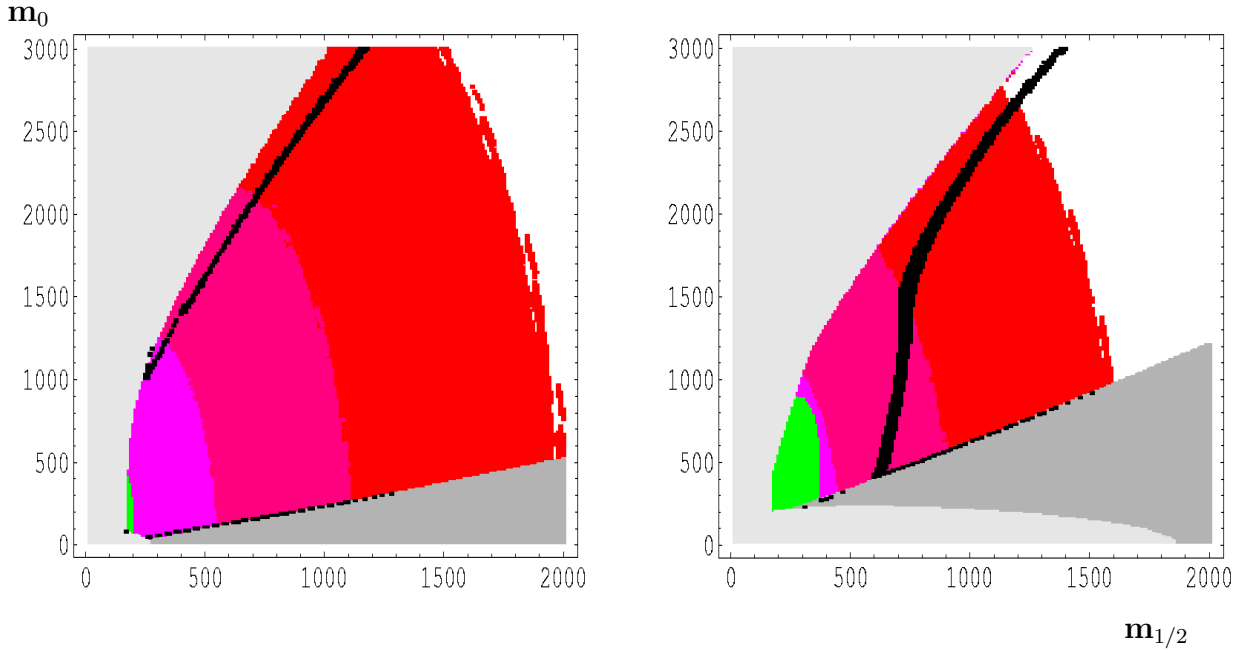


Figure 3: The $mSUGRA$ $(m_{1/2}, m_0)$ parameter space with all constraints imposed for $A_0 = 0, \mu > 0$ and the values $\tan \beta = 10$ (left) and 50 (right). The top quark mass is fixed to $m_t = 166.9$ GeV. Notation and conventions are as in Fig. 1.

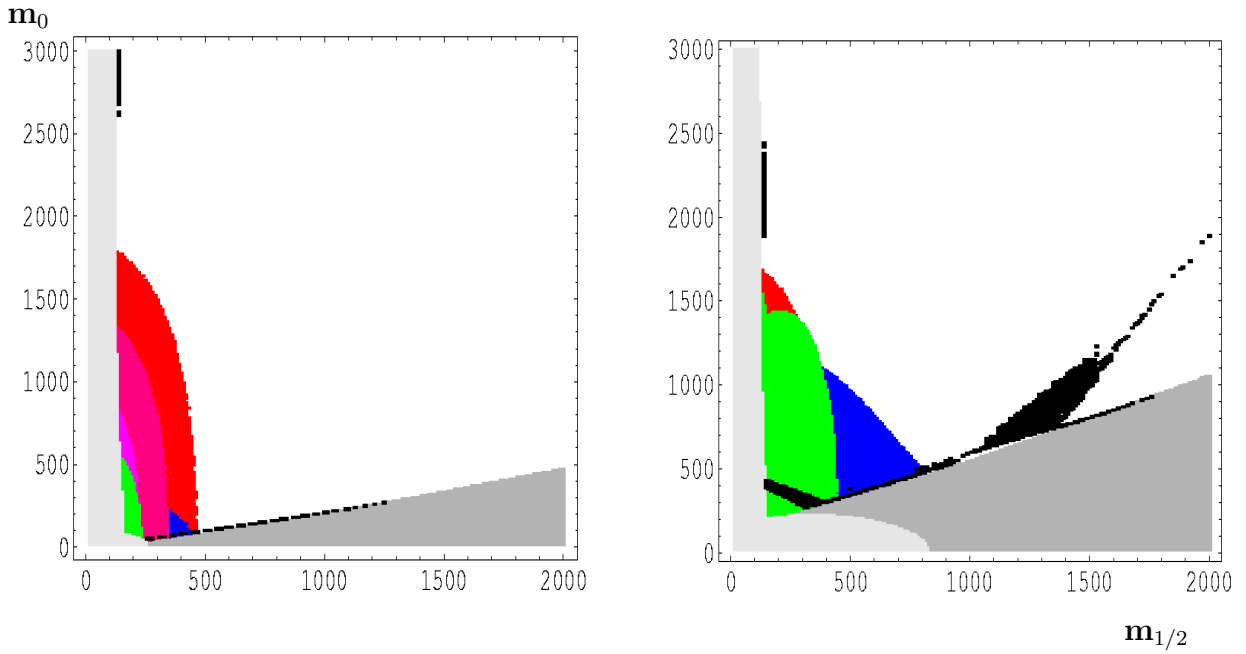


Figure 4: The $mSUGRA$ $(m_{1/2}, m_0)$ parameter space with all constraints imposed for $A_0 = 0, \mu > 0$ and the values $\tan \beta = 10$ (left) and 50 (right). The top quark mass is fixed to $m_t = 178$ GeV. Notation and conventions are as in Fig. 1.

more easily circumvented than the other constraints discussed here.

The excluded grey regions also increase with increasing $\tan\beta$. Increased $\tilde{\tau}_L - \tilde{\tau}_R$ mixing as well as reduced diagonal $\tilde{\tau}$ masses due to RG effects imply that the requirement $m_{\tilde{\tau}_1} > m_{\tilde{\chi}_1^0}$ excludes an increasing area with $m_{1/2}^2 \gg m_0^2$. Similarly, the requirement of correct electroweak symmetry breaking excludes an increasing area at $m_0^2 \gg m_{1/2}^2$. For small values of $\tan\beta$ the increase of this excluded region is mostly due to the reduction of the top Yukawa coupling, which scales like $1/\sin\beta$; for larger $\tan\beta$ the effects of the bottom Yukawa, which scales like $1/\cos\beta \simeq \tan\beta$ for $\tan^2\beta \gg 1$, in the RGE become more important, which to some extent counter-act the contributions of the top Yukawa coupling. For the large value $\tan\beta = 58$ (Fig. 2), this region covers most of the parameter space as the bottom Yukawa coupling becomes very large. For even larger values, $\tan\beta > 58$, one cannot obtain correct electroweak symmetry breaking.

The grey regions also depend very sensitively on the top mass, as shown by Figs. 3 and 4. Figs. 5 and 6 show that increasing $|A_0|$ reduces the region at $m_0^2 \gg m_{1/2}^2$ where one cannot break the electroweak symmetry; on the other hand, a significant region near the origin is now excluded by the false vacuum (“CCB”) constraints.

The (blue) region favored by the measurement of $g_\mu - 2$ (if the SM prediction using data from e^+e^- annihilation can be trusted) also expands towards larger values of m_0 and $m_{1/2}$ as $\tan\beta$ is increased. This region depends only slightly on m_t ; somewhat larger values of m_0 become compatible with this constraint if m_t is reduced. This is due to the reduction of μ caused by reducing m_t . The dependence of this region on A_0 is again rather mild; however, for $A_0 = -2$ TeV the entire blue region is excluded by the $b \rightarrow s\gamma$ constraint.

Finally, for $\tan\beta = 5$ (Fig. 2), the (black) regions satisfying the DM constraint (7) lie right at the border of the theoretically allowed parameter space: the stau co-annihilation region, where $m_{\tilde{\tau}_1} \simeq m_{\tilde{\chi}_1^0}$, lies next to the region excluded by a charged LSP, whereas for small $\tan\beta$ the “focus point region”, where $\mu \lesssim M_1$ at the weak scale, is right next to the region where the electroweak symmetry can no longer be broken. The same holds true for $\tan\beta = 10$ and $m_t = 178$ GeV (Fig. 4), for $\tan\beta = 30$ and $A_0 = -2$ TeV (Fig. 6), and for $\tan\beta = 30$, $A_0 = -1$ TeV and $m_t = 178$ GeV (Fig. 5); in this last case the small black region at $m_0 \gg m_{1/2}$ is allowed due to almost resonant h exchange [43].

However, for larger $\tan\beta$ and/or smaller m_t there are sizable regions of parameter space where the DM relic density comes out too low. This happens in particular for $m_0^2 \gg m_{1/2}^2$, where one can have an almost pure higgsino as LSP once $\tan\beta \gtrsim 10$ (for $m_t = 172.7$ GeV; for smaller m_t this region appears at smaller $\tan\beta$). Comparison of Figs. 1–2 and 3 shows that the lowest values of m_0 in this higgsino–LSP region decreases very quickly with decreasing

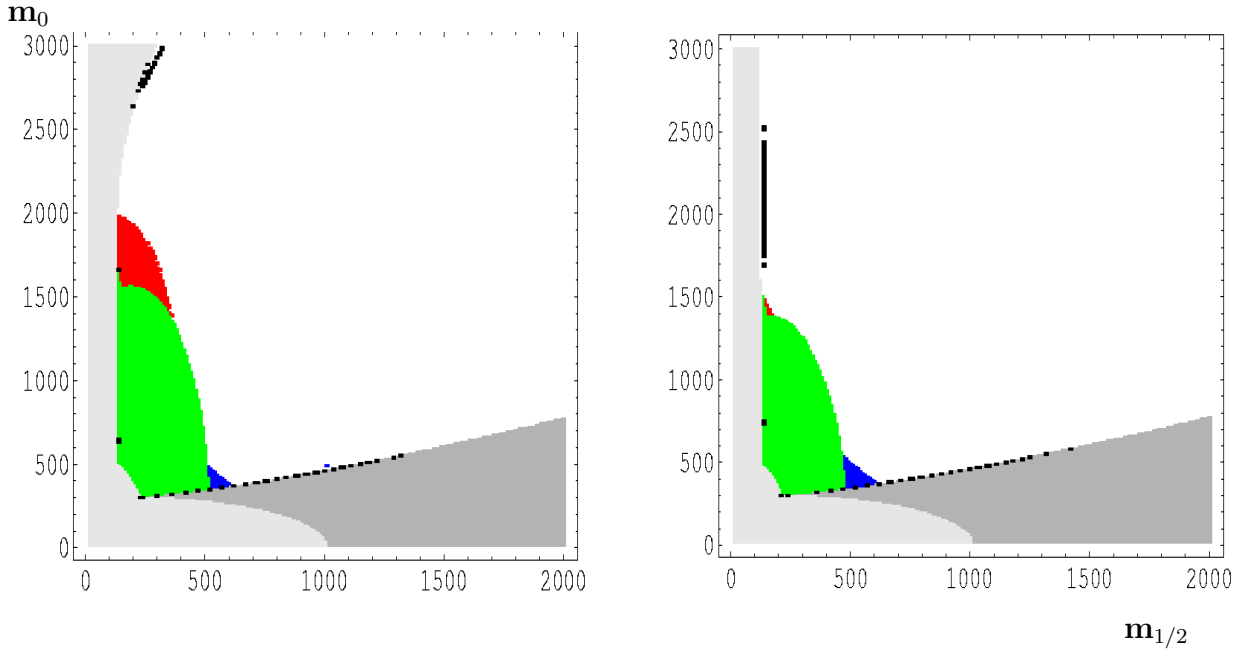


Figure 5: The $mSUGRA$ ($m_{1/2}, m_0$) parameter space with all constraints imposed for $A_0 = -1$ TeV, $\mu > 0$, $\tan\beta = 30$. The top quark mass is fixed to $m_t = 172.7$ (left) and 178 GeV (right). Notation and conventions are as in Fig. 1.

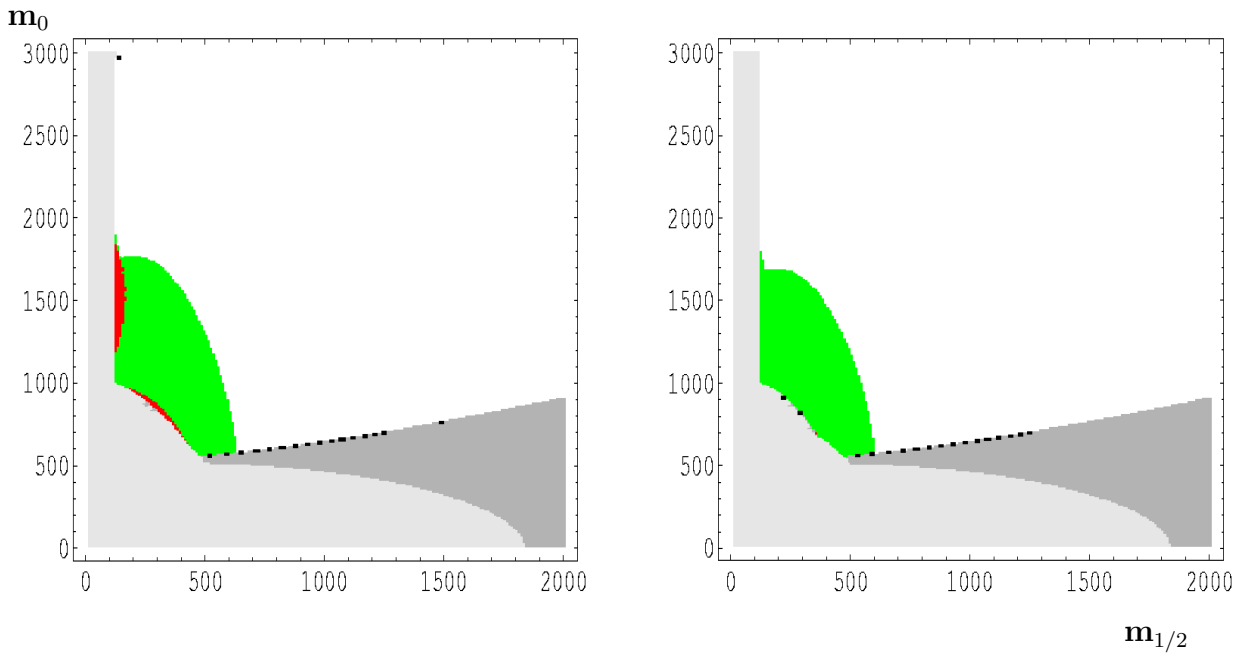


Figure 6: The $mSUGRA$ ($m_{1/2}, m_0$) parameter space with all constraints imposed for $A_0 = -2$ TeV, $\mu > 0$, $\tan\beta = 30$. The top quark mass is fixed to $m_t = 172.7$ (left) and 178 GeV (right). Notation and conventions are as in Fig. 1.

m_t . The reason is that larger m_t imply a smaller (often: more negative) soft breaking contribution to the squared mass of the Higgs boson that couples to the top quark, which in turn implies a larger value of $|\mu|$ via the conditions of electroweak symmetry breaking.

For the same reason, a reduced m_t makes it easier to find solutions with $m_A \simeq 2m_{\tilde{\chi}_1^0}$, yielding the very prominent DM-allowed “ A -pole” region visible for $\tan\beta = 50$ in Figs. 2–4; recall that μ^2 contributes with positive sign to m_A^2 . This region becomes broader with reduced m_t since lower values of $|\mu|$ also mean stronger gaugino–higgsino mixing in the neutralino sector, and hence a larger $\tilde{\chi}_1^0\tilde{\chi}_1^0A$ coupling. For $\tan\beta = 58$ (Fig. 2) m_A is everywhere significantly below $2m_\chi$. The very large $(A, H)b\bar{b}$ couplings nevertheless imply that for moderate values of m_0 and $m_{1/2}$, $\tilde{\chi}_1^0$ annihilation through virtual A and H exchange has the right strength. This DM-allowed region is connected to the A -pole region at smaller (although still large) values of $\tan\beta$. For $\tan\beta = 58$ and small m_0 and $m_{1/2}$, the virtual A, H -exchange contributions even lead to too small a $\tilde{\chi}_1^0$ relic density; however, this region of parameter space is excluded by the $b \rightarrow s\gamma$ constraint.

On the other hand, a reduced top mass of 172.7 GeV also implies that the “bulk” regions, where the DM constraint (7) is satisfied due to the exchange of light sleptons in the t - and u -channel, now lies deep in the region excluded by Higgs searches at LEP. Fig. 4 is a reminder that a bulk region compatible with all constraints (with the possible exception of the theoretically somewhat shaky $b \rightarrow s\gamma$ constraint) still exists for $m_t = 178$ GeV and (sufficiently) large $\tan\beta$. Recall that increasing $\tan\beta$ increases $\tilde{\tau}_L - \tilde{\tau}_R$ mixing, which in turn increases the S -wave LSP annihilation cross section through $\tilde{\tau}$ exchange [44].

Note finally that the additional possible region where the DM constraint could be satisfied, i.e. with co-annihilation of the LSP neutralino with top squarks [45], is disfavored in the mSUGRA scenario that we are discussing here.

It is interesting to note that several indications for “new physics” can be explained simultaneously within mSUGRA. The reduction of the central value of m_t has made it a bit more difficult to satisfy the (aggressive) $g_\mu - 2$ requirement (5), which prefers moderate values of sparticle masses unless $\tan\beta$ is quite large, in potential conflict with the LEP Higgs search limits. However, if we allow a 3 GeV theoretical uncertainty in the calculation of m_h , solutions satisfying (5) can be found for all $\tan\beta \geq 8$ for $m_t = 172.7$ GeV and $A_0 = 0$; if finite values of A_0 are considered, the lower limit on $\tan\beta$ is reduced even further. On the other hand, if we take the prediction of m_h at face value, again taking $m_t = 172.7$ GeV we need $\tan\beta \geq 12$ (7) for vanishing (arbitrary) A_0 ; for $m_t = 166.9$ GeV, as in Fig. 3, these lower bounds increase to 20 and 10, respectively. In all these cases we can satisfy the DM constraint (7) in the $\tilde{\tau}_1$ co-annihilation region, and have a CP-even Higgs boson near 115

GeV, as hinted at by LEP data, while satisfying the $g_\mu - 2$ constraint (5) at the same time.

Fig. 2 shows that these three constraints can also be satisfied simultaneously in the A -pole region, if $\tan\beta$ is very large. However, we did not find any points in the “focus point” region where the aggressive $g_\mu - 2$ constraint can be satisfied, if we take the prediction for m_h at face value. In this case increasing m_t , and/or introducing non-vanishing A_0 , would allow to satisfy the Higgs search limits for smaller values of m_0 , thereby increasing $a_{\mu, \text{SUSY}}$; however, at the same time it would increase $|\mu|$, pushing the $\tilde{\chi}_1^0$ relic density to unacceptably large values. Even if we only demand the calculated m_h to exceed 111 GeV (i.e. assume sizable positive higher order corrections to m_h) one can only reach the lower end of the range (5) in this region of parameter space.

3.2 Parameter space with physical masses

We now present some results for physical masses. In order to keep the number of figures manageable, we only show results for the central value of $m_t = 172.7$ GeV, $A_0 = 0$, and two values of $\tan\beta$.

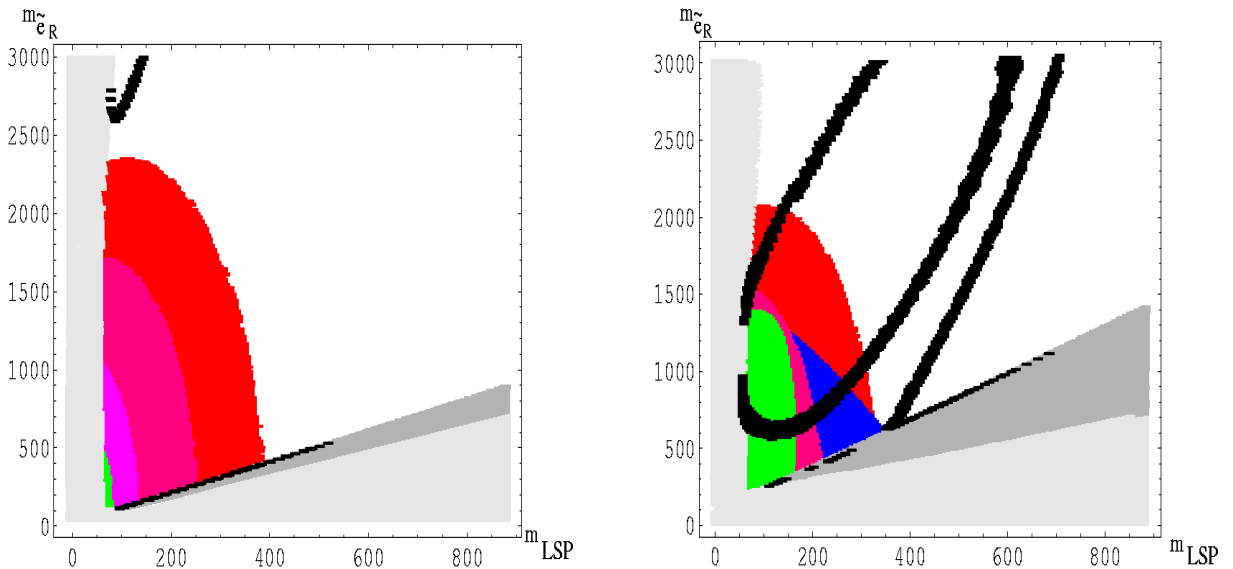


Figure 7: The $mSUGRA$ ($m_{\tilde{\chi}_1^0}, m_{\tilde{e}_R}$) parameter space with all constraints imposed for $A_0 = 0$, $\mu > 0$, $\tan\beta = 10$ (left) and $\tan\beta = 50$ (right). The top mass is fixed to $m_t = 172.7$ GeV. Notations and conventions are as in Fig. 1, except that the light grey region now also includes combinations of masses that are never realized in $mSUGRA$.

We begin with the $(m_{\tilde{\chi}_1^0}, m_{\tilde{e}_R})$ plane depicted in Fig. 7; these masses largely determine the phenomenology of \tilde{e}_R pair production at e^+e^- colliders. These figures actually look

quite similar to the corresponding results in Figs. 1–2. The reason is that over most of mSUGRA parameter space, $\tilde{\chi}_1^0$ is dominated by the Bino component, with $m_{\tilde{\chi}_1^0} \sim 0.4m_{1/2}$, whereas $m_{\tilde{e}_R}^2 \sim m_0^2 + 0.15m_{1/2}^2$ implies that the mass of \tilde{e}_R is usually quite close to m_0 . Note, however, that the excluded region at $m_{\tilde{e}_R}^2 \gg m_{\tilde{\chi}_1^0}^2$ does not grow with increasing $\tan\beta$, in contrast to the analogous region in the $(m_0, m_{1/2})$ plane. The reason is that the boundary⁸ of this region is set by the search limit for (higgsino–like) charginos at LEP, which essentially fixes the mass of $\tilde{\chi}_1^0$, which is also higgsino–like here.

The $(m_{\tilde{g}}, m_{\tilde{u}_L})$ plane is shown in Fig. 8; since the other first and second generation squarks have masses quite close to $m_{\tilde{u}_L}$ this plane essentially determines the cross section for the production of strongly interacting sparticles at hadron colliders [46] (with the possible exception of a light \tilde{t}_1 ; see below). In this case both masses depend significantly on the gaugino mass parameter, with $m_{\tilde{u}_L}^2 \sim m_0^2 + 6m_{1/2}^2$ and $m_{\tilde{g}} \sim 2.5m_{1/2}$. As a result, the accessible part of parameter space gets squeezed, whereas the entire region $m_{\tilde{u}_L} \lesssim 0.8m_{\tilde{g}}$ is not accessible [47], greatly increasing the size of the grey regions compared to the analogous results of Figs. 1–2. Moreover, since $m_{\tilde{g}}$ is independent of μ , the region at $m_{\tilde{u}_L}^2 \gg m_{\tilde{g}}^2$ that is excluded because μ^2 comes out too small does grow with increasing $\tan\beta$. Note that our basic parameter scan only included values of m_0 up to 3 TeV. As a result, the area with $m_{\tilde{u}_L} > 3$ TeV and much smaller $m_{\tilde{g}}$ did not get probed, although some of it is theoretically accessible.

We next turn to the $(m_{\tilde{t}_1}, m_{\tilde{\tau}_1})$ parameter space depicted in Fig. 9. In this case both masses depend significantly on m_0 , but only $m_{\tilde{t}_1}$ has a strong dependence on $m_{1/2}$. The “focus point” region with higgsino–like or mixed LSP is therefore still at the top–left of the accessible region. However, the inaccessible region at the left side of the figure is considerably larger than in Figs. 1–2, since for our choice $A_0 = 0$, one cannot have $m_{\tilde{\tau}_1}$ too much above $m_{\tilde{t}_1}$. Note also that we chose different y –scales in the two frames of Fig. 9. Increasing $\tan\beta$ increases the τ Yukawa coupling, which reduces the soft breaking masses in the $\tilde{\tau}$ sector through RG effects, and increases $\tilde{\tau}_L - \tilde{\tau}_R$ mixing; both effects tend to reduce $m_{\tilde{\tau}_1}$. For $\tan\beta = 10$, $m_{\tilde{\tau}_1}$ is quite close to $m_{\tilde{e}_R}$, but for $\tan\beta = 50$ it is significantly smaller. On the other hand, $m_{\tilde{t}_1}$ is relatively insensitive to $\tan\beta$.

The Higgs sector [48] reflects the radiative symmetry breaking in mSUGRA. For small and moderate values of $\tan\beta$ the heavier Higgs bosons, whose masses are essentially determined by that of the CP–odd Higgs boson A , are among the heaviest of all new particles [49]. On the other hand, for large $\tan\beta$, RG effects due to the bottom Yukawa coupling greatly reduce m_A . We saw in the previous section that this leads to scenarios where $m_A \simeq 2m_{\tilde{\chi}_1^0}$, and hence

⁸Most of this region is excluded since electroweak symmetry breaking would require $\mu^2 < 0$; however, there is also a small area where μ^2 is positive, but below the LEP limit.

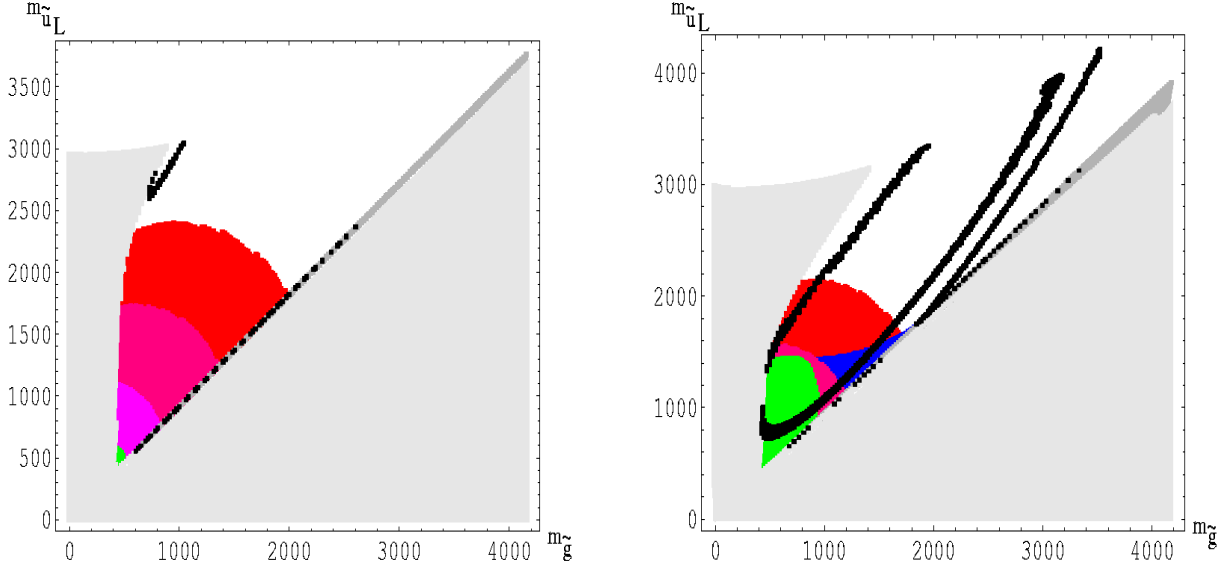


Figure 8: The $mSUGRA$ ($m_{\tilde{g}}, m_{\tilde{u}_L}$) parameter space with all constraints imposed for $A_0 = 0$, $\mu > 0$, $\tan \beta = 10$ (left) and $\tan \beta = 50$ (right). The top mass is fixed to $m_t = 172.7$ GeV.

to strong $\tilde{\chi}_1^0$ annihilation in the early Universe due to near-resonant A boson exchange. This reduction of m_A is reflected by the reduced y -scale in the right frames in Figs. 10 and 12, which show the $(m_{\tilde{\chi}_1^0}, m_A)$ and (m_h, m_A) planes, respectively. In fact, Fig. 10 shows that for $\tan \beta = 10$, m_A is at least 2.5 times larger than the LSP mass, and could be arbitrarily large if very large values of m_0 are included in the scan. On the other hand, for $\tan \beta = 50$, only a very narrow range of m_A values is possible for a given LSP mass, indicating that now m_A has become almost (although not quite) independent of m_0 .

The $(m_{\tilde{\chi}_1^0}, m_h)$ plane is shown in Fig. 11. In the left frame we see that the upper black (DM-allowed) region is also almost horizontal, indicating that in this “focus point” region m_h depends very weakly on $m_{1/2}$. In fact, since we have $m_A^2 \gg m_h^2$ everywhere in this frame, m_h depends on m_0 and $m_{1/2}$ only through loop corrections, in particular through the soft breaking stop masses, which are not sensitive to $m_{1/2}$ as long as $m_0^2 \gg m_{1/2}^2$. Since in Fig. 1 this region covers only a narrow range of m_0 it also corresponds to a narrow range of m_h . On the other hand, in the $\tilde{\tau}_1$ co-annihilation region we have $m_0^2 \ll m_{1/2}^2$, so that the \tilde{t} masses are mostly determined by $m_{1/2}$. Since this region covers a broad range of $m_{1/2}$, it also extends over a significant range of m_h . In this second branch the logarithmic increase of m_h with the SUSY mass scale, here represented by the LSP mass, is clearly visible.

For $\tan \beta = 50$ the four distinct DM-allowed bands shown in the corresponding Figs. 2 or 7 collapse to two bands. The $\tilde{\tau}_1$ co-annihilation band is connected to the band where

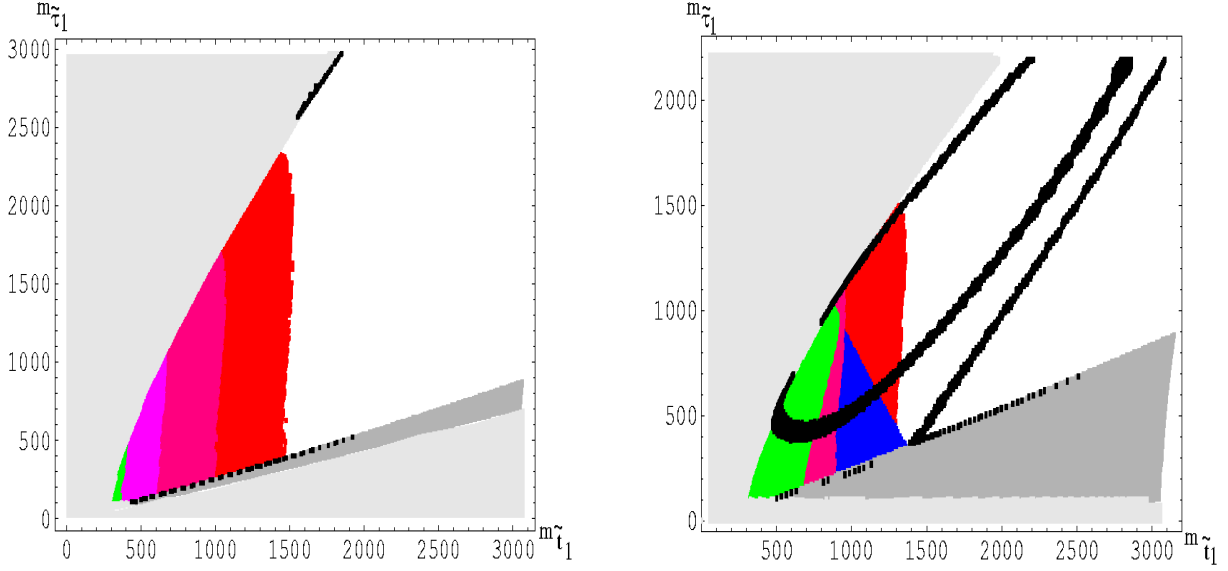


Figure 9: The $mSUGRA$ $(m_{\tilde{t}_1}, m_{\tilde{\tau}_1})$ parameter space with all constraints imposed for $A_0 = 0$, $\mu > 0$, $\tan \beta = 10$ (left) and $\tan \beta = 50$ (right). The top mass is fixed to $m_t = 172.7$ GeV.

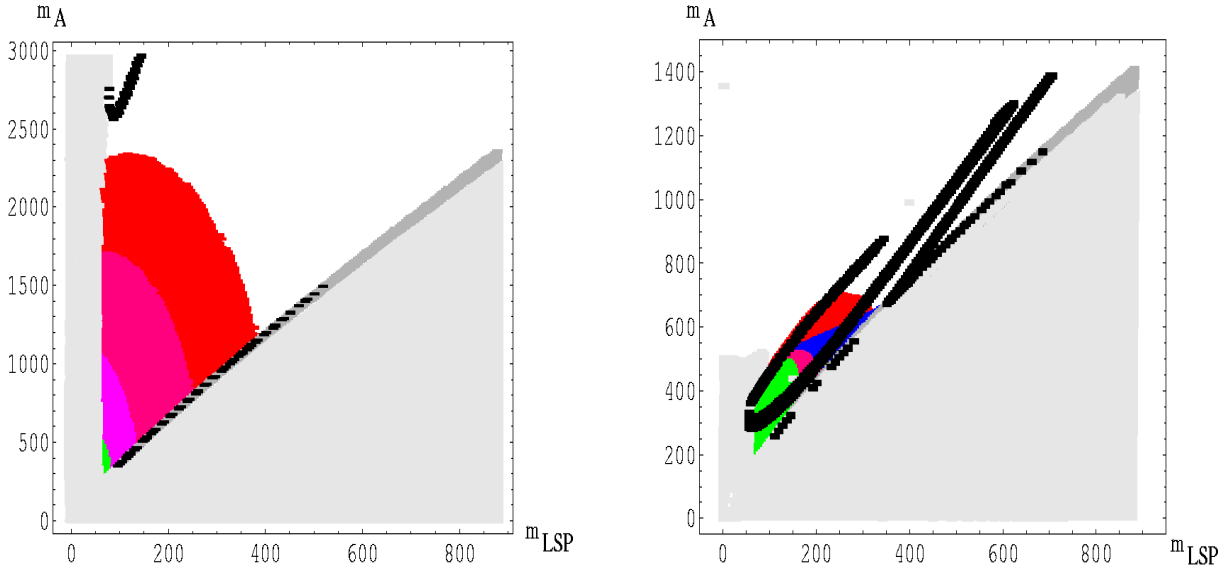


Figure 10: The $mSUGRA$ $(m_{\tilde{\chi}_1^0}, m_A)$ parameter space with all constraints imposed for $A_0 = 0$, $\mu > 0$, $\tan \beta = 10$ (left) and $\tan \beta = 50$ (right). The top mass is fixed to $m_t = 172.7$ GeV.

$2m_{\tilde{\chi}_1^0}$ is slightly above m_A even in the $(m_0, m_{1/2})$ plane. Together with the band where $2m_{\tilde{\chi}_1^0}$ is slightly below m_A , which gives very similar results for m_h , they form the lower black band in Fig. 11. The DM-allowed region with mixed higgsino–bino LSP, which is quite prominent

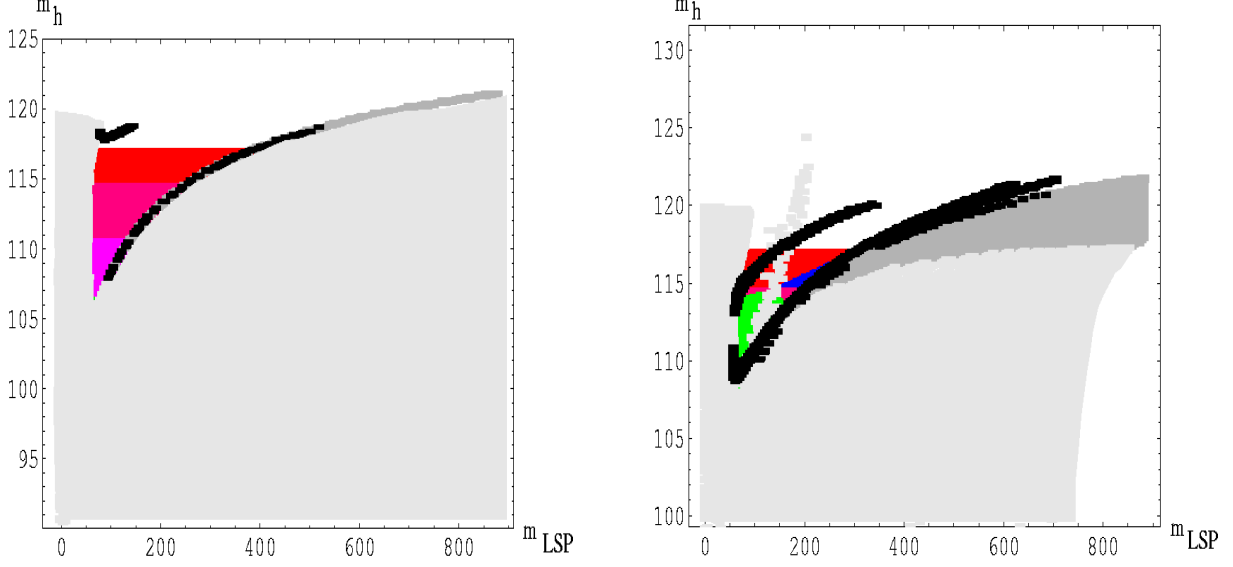


Figure 11: *The $mSUGRA$ $(m_{\tilde{\chi}_1^0}, m_h)$ parameter space with all constraints imposed for $A_0 = 0$, $\mu > 0$, $\tan \beta = 10$ (left) and $\tan \beta = 50$ (right). The top mass is fixed to $m_t = 172.7$ GeV.*

for $\tan \beta = 50$, gives the upper black band in the right frame of Fig. 11. Note also that for fixed $m_{\tilde{\chi}_1^0}$, in the DM-allowed region m_h for $\tan \beta = 50$ exceeds that for $\tan \beta = 10$ only by about 1 GeV. However, in the latter case $m_{\tilde{\chi}_1^0}$ up to ~ 700 GeV can be compatible with the DM constraint, whereas for $\tan \beta = 10$ this requires $m_{\tilde{\chi}_1^0} \lesssim 500$ GeV; the upper bound on m_h in the DM-allowed region therefore grows by about three GeV when $\tan \beta$ is increased from 10 to 50. These results are compatible with those of ref. [20].

Finally, the (m_h, m_A) plane is shown in Fig. 12. The most obvious feature here is the strong correlation of these two Higgs boson masses. In the left frame ($\tan \beta = 10$) the lower black (DM-allowed) strip is the $\tilde{\tau}_1$ co-annihilation region, whereas the upper black strip is the “focus point” region. In the latter part of parameter space $|\mu|$ is relatively small, and effects of the bottom Yukawa coupling are still almost negligible, so that $m_A \simeq m_0$. Moreover, both m_A and m_h are quite insensitive to $m_{1/2}$, so long as $m_0^2 \gg m_{1/2}^2$. This leads to a strong compression of the accessible region, which in this part of parameter space almost coincides with the DM-allowed region. However, the upper black strip in the right frame is surrounded by “inaccessible” light grey regions only because we limited our scan to $m_0 \leq 3$ TeV; otherwise it would be connected by the (experimentally and theoretically allowed, but DM-disfavored) white region.

In the right frame of Fig. 12, i.e. for $\tan \beta = 50$, the *lower* black region is the “focus point” region, whereas the upper black strip is the $\tilde{\tau}_1$ co-annihilation region merged with

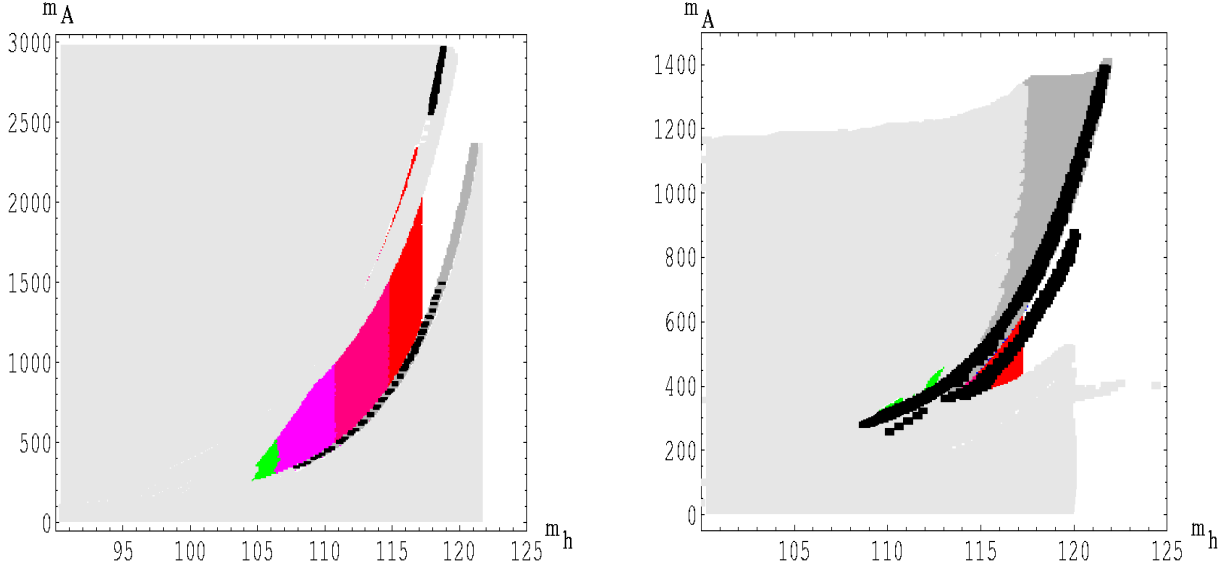


Figure 12: *The $mSUGRA$ (m_h, m_A) parameter space with all constraints imposed for $A_0 = 0$, $\mu > 0$, $\tan \beta = 10$ (left) and $\tan \beta = 50$ (right). The top mass is fixed to $m_t = 172.7$ GeV.*

the A -pole region, as discussed in the context of Fig. 11. For given m_A , m_h is maximized if $m_{1/2}$ is minimized, i.e. in the “focus point” region. The reason is that m_A is sensitive to $m_{1/2}$ already at the tree-level, through the relation that fixes μ^2 in terms of M_Z^2 and the soft breaking parameters; in contrast, if $m_A^2 \gg M_Z^2$, m_h depends on $m_{1/2}$ only through loop effects. We also note that the accessible region of the (m_h, m_A) plane becomes very narrow for large $\tan \beta$.

4. Sparticle and Higgs boson mass bounds

The figures shown in Sec. 3.1 show that the allowed region in the $(m_0, m_{1/2})$ plane depends very strongly on the value of $\tan \beta$. There is also a significant dependence on A_0 . Finally, even though the top mass is now the (relatively) most accurately known of all quark masses, we saw that varying m_t within its current limits still moves the boundaries of allowed regions by hundreds or, in case of the “focus point” region, even thousands of GeV. Similar shifts of the allowed region occur when plotted in terms of pairs of physical masses, as shown in Sec. 3.2.

One simple way to show the *total* allowed ranges of physical masses is to scan over the entire parameter space that is consistent with a given set of constraints; this is the topic of this Section. We saw in Sec. 2 that not all constraints should be treated on an equal footing.

Briefly, lower bounds on masses (or cross sections or branching ratios) from accelerator-based experiments are most robust, since both beam and detector are (hopefully) well controlled by the experimenter. Bounds on masses, and on cross sections of processes that can occur at tree level, usually also do not have many theoretical ambiguities. In contrast, we saw that one can evade the $b \rightarrow s\gamma$ constraint by a relatively minor modification of the model [38]. In the case of the $g_\mu - 2$, there is the additional ambiguity due to the $\sim 2\sigma$ discrepancy between SM ‘predictions’ based on different data sets, see eqs. (4) and (5). Finally, the DM constraint (7) required several (reasonable) assumptions for its derivation, and needs additional assumptions to be translated into allowed regions in the mSUGRA parameter space.

It was originally hoped that the upper bound on the DM relic density (the so-called ‘overclosure’ constraint) would allow to establish reliable, useful upper bounds on sparticle masses. Under the standard assumptions listed in Sec. 2, the predicted LSP relic density is proportional to the inverse of the (effective) LSP annihilation cross section into SM particles (or MSSM Higgs bosons, if kinematically accessible). This cross section in turn (through dimensional arguments, or by unitarity) scales like the inverse square of the relevant mass scale. Indeed, unitarity does allow to establish an upper bound on the mass of any WIMP; however, this bound exceeds 100 TeV [50], and is thus not particularly useful, since we lack the means to build colliders that could cover this kind of mass range. In the context of mSUGRA, it became clear quite early on [44] that very, even “unnaturally”, large masses can be compatible with the DM constraint (7) even in standard cosmology.

On the other hand, we did see in Figs. 1–6 that this constraint excludes large chunks of otherwise allowed parameter space. One might therefore think that it would at least affect the lower bounds on sparticle masses significantly. Table 1 shows that this is not really the case. This table lists lower bounds on the masses of some new (s)particles, imposing various sets of constraints. We always impose all constraints discussed up to and including eq. (4) in Sec. 2. Sets I through III and IV through VI differ in that they are based on the conservative $g_\mu - 2$ constraint (4) and the more aggressive constraint (5), respectively. Since the latter requires a positive supersymmetric contribution to g_μ , it allows us to derive *upper* bounds as well as lower bounds on the masses of new (s)particles. In addition to these basic constraints, sets II and V impose the $b \rightarrow s\gamma$ constraint (6), and sets III and VI in addition impose the DM constraint (7).

We see that the lower bounds on the masses of some key (s)particles always saturate their current bounds from collider physics, no matter what additional constraints we impose. This is true, in particular, for the lighter chargino, the lightest charged slepton (always $\tilde{\tau}_1$

Table 1: Lower bounds on the masses of superparticles and Higgs bosons, and upper bound on the LSP–nucleon scattering cross section, derived in $mSUGRA$ under six different sets of assumptions. “HWIP” and “HSIP” stand for “heaviest weakly interacting particle” and “heaviest strongly interacting particle”, respectively. In all cases the constraints discussed in Sec. 2 up to the requirement (4) are imposed. In Set II we in addition impose the constraint (6) from $b \rightarrow s\gamma$ decays (including the sign of the decay amplitude). Including in addition the DM constraint (7) leads to Set III. Sets IV–VI are like Sets I–III, except that the more conservative $g_\mu - 2$ constraint (4) has been replaced by the more aggressive requirement (5); in these cases we give allowed ranges, rather than only one-sided bounds. (Upper bounds on masses in Set V are the same as in Set IV.) All limits have been obtained by scanning the parameter space (1), for $166.9 \text{ GeV} \leq m_t \leq 178.5 \text{ GeV}$.

Quantity	Set I	Set II	Set III	Set IV	Set V	Set VI
$m_{\tilde{e}_R} \simeq m_{\tilde{\mu}_R}$ [GeV]	106	106	107	[106,1320]	106	[108,1300]
$m_{\tilde{e}_L} \simeq m_{\tilde{\mu}_L}$ [GeV]	152	168	169	[152,1330]	168	[171,1310]
$m_{\tilde{\tau}_1}$ [GeV]	99	99	99	[99,1020]	99	[99,915]
$m_{\tilde{\tau}_2}$ [GeV]	156	171	172	[156,1160]	171	[174,1130]
$m_{\tilde{\nu}_\tau}$ [GeV]	130	149	149	[130,1160]	149	[152,1120]
$m_{\tilde{\chi}_1^\pm}$ [GeV]	105	105	105	[105,674]	105	[105,667]
$m_{\tilde{\chi}_2^\pm}$ [GeV]	218	218	233	[219,1003]	227	[337,999]
$m_{\tilde{\chi}_1^0}$ [GeV]	52	52	53	[52,359]	53	[55,357]
$m_{\tilde{\chi}_2^0}$ [GeV]	105	105	105	[105,674]	105	[106,667]
$m_{\tilde{\chi}_3^0}$ [GeV]	135	135	135	[135,996]	135	[292,991]
$m_{\tilde{\chi}_4^0}$ [GeV]	217	218	234	[218,1003]	226	[337,999]
$m_{\tilde{g}}$ [GeV]	359	380	380	[361,1880]	399	[412,1870]
$m_{\tilde{d}_R} \simeq m_{\tilde{s}_R}$ [GeV]	406	498	498	[406,1740]	498	[498,1740]
$m_{\tilde{d}_L} \simeq m_{\tilde{s}_L}$ [GeV]	424	518	518	[424,1810]	518	[518,1800]
$m_{\tilde{b}_1}$ [GeV]	294	459	463	[295,1520]	459	[463,1500]
$m_{\tilde{b}_2}$ [GeV]	400	498	498	[400,1600]	498	[498,1590]
$m_{\tilde{t}_1}$ [GeV]	102	104	104	[102,1440]	231	[244,1440]
$m_{\tilde{t}_2}$ [GeV]	429	547	547	[431,1600]	547	[547,1590]
m_h [GeV]	91	91	91	[91,124]	91	[91,124]
m_H [GeV]	111	111	111	[111,975]	111	[111,954]
m_{H^\pm} [GeV]	128	128	128	[128,979]	128	[128,960]
m_{HWIP} [GeV]	349	362	366	[351,1330]	366	[371,1310]
m_{HSIP} [GeV]	432	556	556	[432,1880]	556	[566,1870]
$\sigma_{\tilde{\chi}_1^0 p}$ [ab]	140	140	7.5	[10^{-4} ,140]	140	[10^{-4} ,7.5]

in $mSUGRA$), as well as both the CP–even Higgs bosons. The lower bound on the masses of the charged Higgs boson is also independent of the constraints imposed; it follows almost directly from the structure of the MSSM. The lower bounds on the masses of the gluino and

the lighter two neutralinos are to a large extent fixed by gaugino mass unification and the chargino mass bound. In particular, the bound on $m_{\tilde{\chi}_2^0}$ is practically identical to that on $m_{\tilde{\chi}_1^\pm}$. Note that gaugino mass unification holds for running ($\overline{\text{DR}}$) masses. Going to the pole mass entails potentially quite substantial radiative corrections in case of the gluino [51]. The lower bound on $m_{\tilde{g}}$ therefore increases by about 15% when going from the loosest constraints (Set I) to the tightest ones (Set VI), the biggest increase being due to the $b \rightarrow s\gamma$ constraint, which excludes scenarios with large $\tan\beta$ and relatively small squark masses.

The same effect is also visible in the lower bounds on first and second generation squark masses themselves, which increase by about 20% when this constraint is imposed. Note that even for the loosest set of constraints, Set I, the lower bounds on the masses of first and second generation squarks are significantly above current search limits [27]. This is a consequence of the assumed universality of scalar masses, together with the requirement of having sufficiently large soft breaking masses in the stop sector to satisfy the Higgs search limits. These bounds are therefore saturated for the largest possible m_t value.

The masses of the heavier neutralinos and charginos also depend only weakly on the set of constraints imposed. Most of these lower bounds again follow directly from the structure of the MSSM with gaugino mass unification, together with the LEP bound on $m_{\tilde{\chi}_1^\pm}$; the universality of scalar masses and A -parameters, which are defining properties of mSUGRA, play little role here. The only significant exception is the increase of $m_{\tilde{\chi}_3^0}$ for the most restrictive set of constraints (Set VI). This bound is saturated in the “focus point” region of large m_0 , where the supersymmetric contribution to $g_\mu - 2$ tends to be below the range (5).

The lower bounds on the masses of third generation squarks are the quantities that are most sensitive to the additional constraints imposed in Sets II through VI. In particular, requiring both the more aggressive $g_\mu - 2$ constraint (5) and the $b \rightarrow s\gamma$ constraint (6) more than doubles the lower bound on $m_{\tilde{t}_1}$, from the LEP limit of ~ 100 GeV that can be saturated for Sets I through IV, to about 240 GeV. Combinations of parameters leading to a light \tilde{t}_1 which are compatible with the $b \rightarrow s\gamma$ constraint have relatively small $\tan\beta$, but large m_0 ; this leads to a supersymmetric contribution to $g_\mu - 2$ below the range (5). One can also generate a light \tilde{t}_1 by taking modest values of m_0 and $m_{1/2}$, in agreement with the aggressive $g_\mu - 2$ constraint (5); however, this requires very large values of $|A_0|/m_0$, which leads to a violation of the $b \rightarrow s\gamma$ constraint (6). This latter constraint by itself also increases the lower bound on $m_{\tilde{b}_1}$ by about 50%, since a light \tilde{b}_1 requires large $\tan\beta$ (which maximizes the bottom Yukawa coupling, as well as $\tilde{b}_L - \tilde{b}_R$ mixing), which in turn leads to large (negative, for $\mu > 0$) supersymmetric contributions to $b \rightarrow s\gamma$ decays.

In contrast, imposing in addition the DM constraint (7) has very little effect on the lower

bounds on sparticle masses. It does, however, drastically reduce the maximal possible elastic spin-independent LSP-proton scattering cross section, which is shown in the last line of the Table. The calculation of this cross section is based on refs. [52]. In mSUGRA the potentially largest contributions come from the exchange of the heavier CP-even Higgs boson. Since increasing $\tan\beta$ both reduces the mass of this boson and increases its coupling to down-type quarks, the cross section grows quickly when $\tan\beta$ becomes larger. In addition, it is maximized by increasing the coupling of the LSP to Higgs bosons, which requires rather larger gaugino-higgsino mixing; this cross section is therefore largest in the “focus point” region [53]. However, the same coupling also leads to too effective LSP annihilation, resulting in too low a relic density. Imposing the lower bound on the relic density in (7) therefore reduces the upper bound on this cross section by about a factor of 20. We should mention here that even the reduced value of 7.5 ab, which is saturated for an LSP mass near 160 GeV, exceeds the current experimental lower limit on this quantity, if standard assumptions about the distribution of the LSPs in the halo of our galaxy are correct [54]. Due to the uncertainties in this distribution we have not included LSP search limits in our set of constraints.

While all sets of constraints allow the masses of some weakly interacting sparticles to lie right at the current experimental limit, mSUGRA implies that the *heaviest* weakly interacting new particle (sparticle or Higgs boson) must lie above ~ 350 GeV at least. Note that this limit lies well above the lower bound on the mass of any one weakly interacting (s)particle. The reason is that these bounds cannot be saturated simultaneously. For example, the lower bounds on slepton masses are saturated at moderate values of $\tan\beta$, big enough to avoid excessive lower bounds from Higgs searches, but not so big as to imply strong lower bounds from the $g_\mu - 2$ constraint (4). In contrast, the lower bounds on the masses of the heavy Higgs bosons are saturated at very large values of $\tan\beta$. Similarly, the lower bound on the mass of the heaviest strongly interacting sparticle in a given spectrum is somewhat larger than the largest lower bound considered separately.

As mentioned earlier, imposing the aggressive $g_\mu - 2$ constraint (5) allows to derive *upper* bounds in the masses of sparticles and Higgs bosons. The reason is that the supersymmetric contribution, which comes from gaugino-slepton loops, would vanish if either the gaugino masses or the slepton masses became very large. This leads to upper bounds on both m_0 and $m_{1/2}$, as can be seen by studying the blue regions in Figs. 1 through 6. This in turn imposes an upper bound on $|\mu|$ via the condition of radiative electroweak symmetry breaking. As a result, *all* sparticle and Higgs masses can be bounded in mSUGRA using this single constraint! We emphasize that one needs to assume universality of both scalar and gaugino masses to derive these constraints. Numerically, the upper bounds on the masses of the first

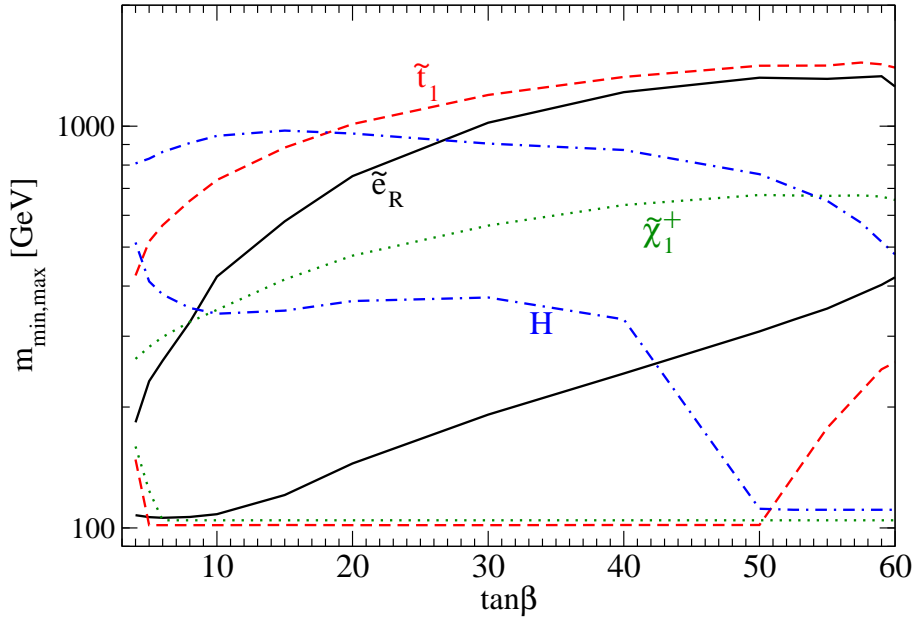
generation squarks as well as on the gluino mass imply that discovery of supersymmetry at the LHC should be straightforward [55]. Unfortunately even in this favorable scenario discovery of charginos would not be guaranteed even at a 1 TeV e^+e^- collider, and discovery of sleptons would be guaranteed only at a CLIC-like machine operating at $\sqrt{s} \gtrsim 3$ TeV. On the other hand, imposing this constraint reduces the upper bound on m_h to 124 GeV (which becomes 127 GeV if one allows for a 3 GeV theoretical uncertainty), which might perhaps even give the Tevatron a chance to probe this scenario (with probably less than compelling statistical significance, alas) [56]. Imposing in addition the $b \rightarrow s\gamma$ constraint does not change these upper bounds at all; even imposing the DM constraint (7) leaves these upper bounds almost unchanged.

One lesson from Table 1 is that imposing the DM constraint (7) has little effect on either upper or lower bounds on the masses of sparticles and Higgs bosons in mSUGRA, *if* one scans over the entire allowed parameter space. Figs. 13 show that the dramatic reduction of the allowed region that results from this constraint that is evident in the Figures presented in Sec. 3 does narrow down the possible ranges of masses when $\tan\beta$ is kept fixed. These figures compare the allowed ranges of the masses of \tilde{e}_R , $\tilde{\chi}_1^\pm$, \tilde{t}_1 and H for the constraint Sets IV and VI of Table 1. In the former case one can saturate the LEP limit on the mass of the lighter chargino for any $\tan\beta \geq 5$. However, light charginos are DM-compatible only in the “focus point” region, which in turn is (barely) compatible with the $g_\mu - 2$ constraint (5) only at large $\tan\beta$. Moreover, at very large $\tan\beta$ the $b \rightarrow s\gamma$ constraint becomes quite severe. As a result, constraint Set VI allows to saturate the LEP chargino mass bound only for $40 \lesssim \tan\beta \lesssim 50$.

The combined effect of the DM and $b \rightarrow s\gamma$ constraints on the lower bound on $m_{\tilde{t}_1}$ is even more dramatic. Without these constraints, the LEP limit on this mass can be saturated for any $\tan\beta \leq 50$. However, as we already saw in Table 1, the $b \rightarrow s\gamma$ constraint increases the lower bound on this mass bound by more than a factor of 2, if one insists on the aggressive $g_\mu - 2$ constraint (5); Fig. 13 shows that this lower bound then also increases quite rapidly with increasing $\tan\beta$. As a result, if $\tan\beta$ was known, imposing constraint Set VI would allow to predict $m_{\tilde{t}_1}$ to within a factor of ~ 3 . However, since the allowed band moves upward with increasing $\tan\beta$, we can currently predict $m_{\tilde{t}_1}$ only within a factor of ~ 6 , even if we impose this most restrictive set of constraints, as shown in Table 1.

Imposing the DM constraint (7) reduces the upper bounds on sparticle masses for fixed $\tan\beta$. This effect is quite mild in most cases, but becomes prominent for \tilde{e}_R at small and moderate values of $\tan\beta$. The $g_\mu - 2$ constraint (5) by itself already leads to a strong $\tan\beta$ dependence of this bound; recall that the supersymmetric contribution to this quantity is

Set IV: $g_\mu - 2$ from e^+e^- data, no DM constraint



Set VI: $g_\mu - 2$ from e^+e^- data, including $b \rightarrow s\gamma$ and DM constraints

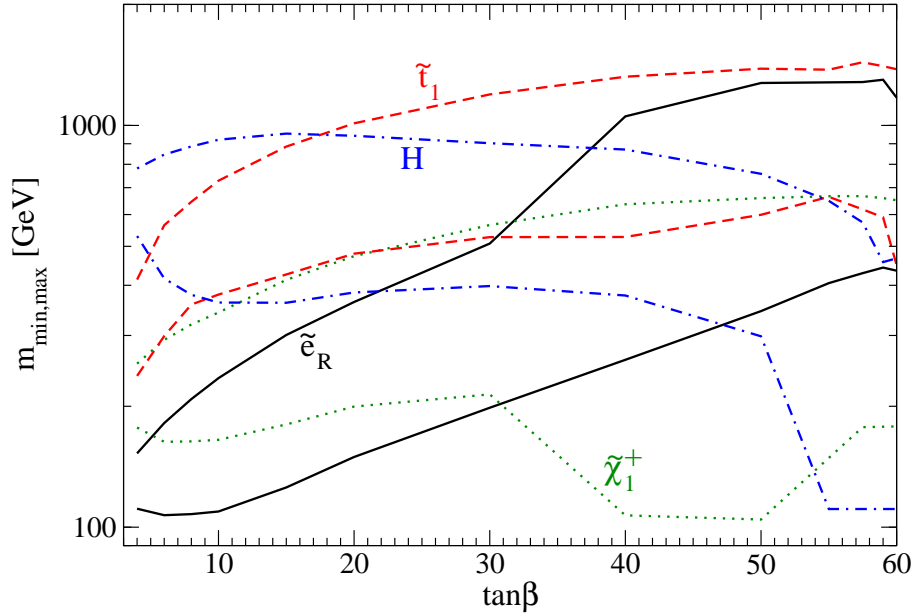


Figure 13: The minimal and maximal value of select particle and Higgs masses: solid (black) curves: \tilde{e}_R ; dashed (red) curves: \tilde{t}_1 ; dotted (green) curves: $\tilde{\chi}_1^\pm$; dot-dashed (blue) curves: H . The upper (lower) figure shows the bounds without (with) imposing the DM and $b \rightarrow s\gamma$ constraints.

essentially proportional to $\tan\beta$. We saw at the end of Sec. 3.1 that for small and moderate $\tan\beta$ the only overlap of the DM and (aggressive) $g_\mu - 2$ allowed regions occurs in the $\tilde{\tau}$ co-annihilation region, which has relatively large gaugino masses; as a result, one needs even smaller slepton masses to produce a sufficiently large $g_\mu - 2$. However, once $\tan\beta \geq 40$, one can satisfy this last constraint even in the “focus point” region; imposing the DM constraint then has little effect on the upper bound on $m_{\tilde{e}_R}$. Finally, we note that the allowed range of m_H is fixed almost completely by the “base” set of constraints plus the aggressive $g_\mu - 2$ constraint (5); imposing in addition the $b \rightarrow s\gamma$ and DM constraints has little effect here.

5. Summary and Conclusions

In this paper we provide an updated scan of the mSUGRA parameter space. This includes the new central value of the mass of the top quark, the inclusion of additional higher order corrections to the mass of the lightest CP-even Higgs boson h , and new information on the sign of the matrix element for $b \rightarrow s\gamma$ decays from the analysis of $b \rightarrow s\ell^+\ell^-$ decays.

We find that the reduction of the central value of m_t from 178 GeV to about 173 GeV shifts the allowed parameter space significantly. This is the consequence of two effects:

- The corrections to m_h^2 scale like the fourth power of m_t , but only scale logarithmically with the sparticle (mostly stop) mass scale. As a result, a few percent reduction of m_t has to be compensated by an increase of $m_{\tilde{t}}$ of up to several tens of percent. This relative shift increases with $m_{\tilde{t}}$, and is therefore most prominent for smaller $\tan\beta$, where the LEP Higgs search constraint is most severe.
- The location of the “focus point” region at $m_0^2 \gg m_{1/2}^2$ where the LSP acquires a significant higgsino component depends very sensitively on m_t . The higgsino component of $\tilde{\chi}_1^0$ is only sizable if $|\mu|$ is rather small. This will happen if the squared soft breaking mass of the Higgs boson coupling to the top quark is small or positive at the “weak” scale Q_W , which should be chosen close to $\sqrt{m_{\tilde{t}_1}m_{\tilde{t}_2}}$ to get good convergence of the perturbative series. This parameter in turn can be written as

$$m_{H_u}^2(Q_W) = am_0^2 + bm_{1/2}^2 + cA_0^2 + dA_0m_{1/2}, \quad (8)$$

where the dimensionless coefficients a, b, c, d depend on the dimensionless MSSM couplings as well as (logarithmically) on Q_W . The crucial observation is that $|a| \ll 1$ for $m_t \sim 175$ GeV and not too small $\tan\beta$ (recall that the top Yukawa coupling at the weak scale is $\propto 1/\sin\beta$). In contrast, $|b|$ is quite sizable, with $b < 0$. A small $m_{H_u}^2(Q_W)$

is therefore only possible if $m_0^2 \gg m_{1/2}^2$ and $a \geq 0$. Since a depends (roughly) quadratically on $m_t/\sin\beta$, but only logarithmically on the sparticle mass scale (through Q_W), a small change of m_t therefore leads to a large shift of the value of Q_W , or, equivalently, of m_0 where the “focus point” region starts.

The first effect makes it more difficult to reconcile, at low values of $\tan\beta$, the Higgs mass constraint from LEP with the evidence for a positive contribution to the anomalous magnetic moment of the muon. However, for larger $\tan\beta$ the Higgs mass bound allows smaller sparticle masses, while the contribution to $g_\mu - 2$ remains significant for larger sparticle masses. As a result, even for $m_t = 173$ GeV both constraints can be satisfied simultaneously for $\tan\beta \gtrsim 10$.

By far the most stringent constraint on the parameter space comes from the requirement that the lightest neutralino should have the correct relic density. As discussed in Sec. 2, this constraint can only be translated into bounds on the mSUGRA parameter space if several assumptions are made. Under the usual assumption of thermal LSP production and standard cosmology, only a few discrete “DM allowed” regions survive. Out of these, the “bulk” region of moderate m_0 and moderate $m_{1/2}$ is affected most by the reduced mass of the top quark; in fact, it disappears altogether if m_t is indeed near its current central value of ~ 173 GeV. The $\tilde{\tau}_1$ co-annihilation region is also reduced in size, since the region excluded by Higgs searches now extends to larger values of $m_{1/2}$. On the other hand, as noted above, the region where the LSP has significant higgsino component becomes *larger* when m_t is reduced. Similarly, the lowest value of $\tan\beta$ where $2m_{\tilde{\chi}_1^0} \simeq m_A$ (the A -pole region) becomes smaller; this region also becomes broader, thanks to the increased strength of the $A\tilde{\chi}_1^0\tilde{\chi}_1^0$ coupling. In contrast, the conceptually similar h -pole region is much reduced in size.

We also provided views of the mSUGRA parameter space plotted in the plane spanned by two physical sparticle or Higgs boson masses. Whereas some masses are essentially independent of each other (e.g. $m_{\tilde{e}_R}$ and $m_{\tilde{\chi}_1^0}$), others are strongly correlated (e.g. m_A and m_h); most pairs are intermediate between these extremes.

In addition to these scans of parameter space, we also provided upper and lower *bounds* on the masses of Higgs bosons and sparticles. Here it is crucial to properly include the uncertainty of the input parameters, in particular, of m_t . This sensitivity comes mostly through the dimensionless coefficients in eq.(8), as well as the analogous expression for $m_{H_d}^2$. These coefficients determine $|\mu|$ through the condition of electroweak symmetry breaking, which affects the spectra of neutralinos, charginos and Higgs bosons. The latter is also directly dependent on these coefficients; through the Higgs search limits, they then affect (the lower bounds on) all sparticle masses. It should be noted that these coefficients also depend on other input parameters, in particular on α_S and m_b . However, this dependence is

much milder than that on m_t . We therefore believe that varying m_t over its entire currently allowed 2σ range, while keeping α_S and m_b fixed to their default values, gives a reasonable estimate of the effect of the current input parameter uncertainties.

The somewhat surprising result of these scans is that the masses of many superparticles and Higgs bosons can still lie right at their current limits from collider searches even if the most restrictive set of constraints is applied, including the Dark Matter constraint and the more aggressive interpretation of the $g_\mu - 2$ constraint. This means that ongoing and near-future experiments still have good chances to discover new particles even in this very constrained version of the MSSM. Not all these lower bounds can be saturated simultaneously, however. As a result, the most robust constraints (essentially the collider limits plus a conservative version of the $g_\mu - 2$ constraint, with no DM requirement) by themselves already imply that a 500 GeV linear collider will not be able to discover all new weakly interacting (s)particles; one will need an energy of at least ~ 700 GeV to achieve this. We also saw that these lower bounds are in most cases surprisingly insensitive to the introduction of new constraints; in particular, requiring the lightest neutralino to be a good thermal DM candidate does not shift them much.

Useful upper bounds on the masses of sparticles and Higgs bosons (with the exception of the lightest CP-even Higgs boson, see ref. [13]) can only be derived if we assume that a positive supersymmetric contribution to $g_\mu - 2$ is indeed required, as is indicated (at the $\sim 2.5\sigma$ level) when data from $e^+e^- \rightarrow$ hadrons are used to calculate the SM prediction for this quantity. This imposes upper bounds on the masses of both sleptons and gauginos; in the mSUGRA context this implies upper bounds on both m_0 and $m_{1/2}$, which leads to upper bounds on *all* new (s)particles. Quantitatively, we find that this requirement by itself implies that strongly interacting sparticles must be within the reach of the LHC. Moreover, a ~ 1 TeV e^+e^- collider would then be able to at least discover superparticles, in the $\tilde{\chi}_1^0\tilde{\chi}_2^0$ channel. However, even in this case one may need a CLIC-like collider, with center of mass energy nearly reaching 3 TeV, to discover all new weakly interacting (s)particles. We stress again that these (upper) bounds have been obtained by scanning over the entire parameter space, including scanning over the 2σ range of m_t . Imposing in addition the Dark Matter constraint narrows down the allowed ranges of some masses if $\tan\beta$ is held fixed, but has little effect on the absolute upper bounds after scanning over the entire allowed parameter space.

We conclude that mSUGRA remains viable. In fact, even after imposing all plausible experimental and theoretical constraints the allowed parameter space still contains a large variety of different spectra, with quite different phenomenology. Even if supersymmetry

provides the missing Dark Matter in the Universe and explains the possible excess of the anomalous dipole moment of the muon, superparticles might be out of reach of both the Tevatron and the first stage of a linear e^+e^- collider; on the other hand, it is also entirely possible that their discovery is “just around the corner”.

Acknowledgments

MD thanks the Center of Theoretical Physics at Seoul National University, as well as the School of Physics at KIAS, for hospitality while this project was nearing completion.

References

- [1] A.H. Chamseddine, R. Arnowitt and P. Nath, Phys. Rev. Lett. **49** (1982) 970; R. Barbieri, S. Ferrara and C.A Savoy, Phys. Lett. **B119** (1982) 343; L. Hall, J. Lykken and S. Weinberg, Phys. Rev. **D27** (1983) 2359; E. Cremmer, P. Fayet and L. Girardello, Phys. Lett. **B122**, 41 (1983); N. Ohta, Prog. Theor. Phys. **70**, 542 (1983).
- [2] H.P. Nilles, Phys. Rep. **110** (1984) 1.
- [3] E. Witten, Nucl. Phys. **B188**, 513 (1981); N. Sakai, Z. Phys. **C11**, 153 (1981); S. Dimopoulos and H. Georgi, Nucl. Phys. **B193**, 150 (1981); R.K. Kaul and P. Majumdar, Nucl. Phys. **B199**, 36 (1982).
- [4] J. Ellis , S. Kelley and D.V. Nanopoulos, Phys. Lett. **B260** (1991) 131; U. Amaldi, W. de Boer and H. Fürstenau, Phys. Lett. **B260** (1991) 447; P. Langacker and M. Luo, Phys. Rev. **D44** (1991) 817; C. Giunti, C.W. Kim and U.W. Lee, Mod. Phys. Lett. **A6** (1991) 1745.
- [5] H. Goldberg, Phys. Rev. Lett. **50**, 1419 (1983); J. Ellis, J. Hagelin, D.V. Nanopoulos, K. Olive and M. Srednicki, Nucl. Phys. **B238**, 453 (1984).
- [6] For a review, see G. Jungman, M. Kamionkowski and K. Griest, Phys. Rep. **267** (1996) 195, hep-ph/9506380.
- [7] L.E. Ibáñez and G.G. Ross, Phys. Lett. **110B**, 215 (1982); L.E. Ibáñez, Phys. Lett. **118B**, 73 (1982); J. Ellis, D.V. Nanopoulos and K. Tamvakis, Phys. Lett. **121B**, 123 (1983); L. Alvarez-Gaumé, J. Polchinski and M.B. Wise, Nucl. Phys. **B221**, 495 (1983).
- [8] D. Auto, H. Baer, C. Balazs, A. Belyaev, J. Ferrandis and X. Tata, JHEP **0306**, 023 (2003), hep-ph/0302155; R. Dermisek, S. Raby, L. Roszkowski and R. Ruiz De

- Austri, JHEP **0304**, 037 (2003), hep-ph/0304101; M.R. Ramage, Nucl. Phys. **B720**, 137 (2005), hep-ph/0412153.
- [9] J.R. Ellis, T. Falk, K.A. Olive and Y. Santoso, Nucl. Phys. **B652**, 259 (2003), hep-ph/0210205; D. Auto, H. Baer, A. Belyaev and T. Krupovnickas, JHEP **0410**, 066 (2004), hep-ph/0407165; H. Baer, A. Belyaev, T. Krupovnickas and A. Mustafayev, JHEP **0406**, 044 (2004), hep-ph/0403214; H. Baer, A. Mustafayev, S. Profumo, A. Belyaev and X. Tata, Phys. Rev. **D71**, 095008 (2005), hep-ph/0412059; G. Bélanger, F. Boudjema, A. Cottrant, A. Pukhov and A. Semenov, Nucl. Phys. **B706**, 411 (2005), hep-ph/0407218, and hep-ph/0412309; J.R. Ellis, K.A. Olive, Y. Santoso and V.C. Spanos, Phys. Lett. **B603**, 51 (2004), hep-ph/0408118; H. Baer, A. Mustafayev, E.-K. Park and S. Profumo, JHEP **0507**, 046 (2005), hep-ph/0505227; Y. Mambrini and E. Nezri, hep-ph/0507263; H. Baer, T. Krupovnickas, A. Mustafayev, E.-K. Park, S. Profumo and X. Tata, hep-ph/0511034.
- [10] J.R. Ellis, K.A. Olive, Y. Santoso and V.C. Spanos, Phys. Lett. **B573**, 162 (2003), hep-ph/0305212, and Phys. Rev. **D70**, 055005 (2004), hep-ph/0405110.
- [11] WMAP Collab., D.N. Spergel et al., Astrophys. J. Suppl. **148**, 175 (2003), astro-ph/0302209.
- [12] H. Baer, C. Balazs, A. Belyaev, J.K. Mizukoshi, X. Tata and Y. Wang, JHEP **0207**, 050 (2002), hep-ph/0205325; H. Baer and C. Balazs, JCAP **0305**, 006 (2003), hep-ph/0303114; U. Chattopadhyay, A. Corsetti and P. Nath, Phys. Rev. **D68**, 035005 (2003), hep-ph/0303201; J.R. Ellis, K.A. Olive, Y. Santoso and V.C. Spanos, Phys. Lett. **B565**, 176 (2003), hep-ph/0303043; M. Battaglia, A. De Roeck, J.R. Ellis, F. Gianotti, K.A. Olive and L. Pape, Eur. Phys. J. **C33**, 273 (2004), hep-ph/0306219; R. Arnowitt, B. Dutta and B. Hu, hep-ph/0310103; J.R. Ellis, K.A. Olive, Y. Santoso and V.C. Spanos, Phys. Rev. **D69**, 095004 (2004), hep-ph/0310356; M.E. Gomez, T. Ibrahim, P. Nath and S. Skadhauge, Phys. Rev. **D70**, 035014 (2004), hep-ph/0404025; J.R. Ellis, S. Heinemeyer, K.A. Olive and G. Weiglein, JHEP **0502**, 013 (2005), hep-ph/0411216.
- [13] B.C. Allanach, A. Djouadi, J.L. Kneur, W. Porod and P. Slavich, JHEP **0409**, 044 (2004), hep-ph/0406166, and references therein.
- [14] CDF Collab. and D0 Collab. and The Tevatron Electroweak Working Group, hep-ex/0507091.

- [15] P. Gambino, U. Haisch and M. Misiak, Phys. Rev. Lett. **94**, 061803 (2005), hep-ph/0410155.
- [16] See e.g. the talk by K. Melnikov at *SUSY2004*, Tsukuba, Japan, June 2004.
- [17] Muon $g-2$ Collab., G.W. Bennett et al., Phys. Rev. Lett. **89**, 101804 (2002), Erratum-
ibid. **89**, 129903 (2002), hep-ex/0208001, and Phys. Rev. Lett. **92**, 161802 (2004),
hep-ex/0401008.
- [18] M. Davier, S. Eidelman, A. Höcker and Z. Zhang, Eur. Phys. J. **C31**, 503 (2003),
hep-ph/0308213; K. Hagiwara, A.D. Martin, D. Nomura and T. Teubner, Phys. Rev.
D69, 093003 (2004), hep-ph/0312250; J.F. de Troconiz and F.J. Yndurain, Phys.
Rev. **D71**, 073008 (2005), hep-ph/0402285; M. Passera, J. Phys. **G31**, R75 (2005),
hep-ph/0411168.
- [19] B.C. Allanach and C.G. Lester, hep-ph/0507283.
- [20] J. Ellis, D. Nanopoulos, K.A. Olive and Y. Santoso, hep-ph/0509331.
- [21] M. Drees and S.P. Martin, in *Electroweak symmetry breaking and new physics at the
TeV scale*, ed. T.L. Barklow, hep-ph/9504324.
- [22] A. Djouadi, M. Drees and J.L. Kneur, JHEP **0108**, 055 (2001), hep-ph/0107316.
- [23] A. Djouadi, J.L. Kneur and G. Moultaka, hep-ph/0211331. The program can be down-
loaded from the web site: www.lpta.univ-montp2.fr/~kneur/Suspect.
- [24] S.P. Martin and M. Vaughn, Phys. Rev. **D50**, 2282 (1994), hep-ph/9311340; I. Jack,
D.R.T. Jones, S.P. Martin, M. Vaughn and Y. Yamada, Phys. Rev. **D50**, 5481 (1994),
hep-ph/9407291.
- [25] J.M. Frère, D.R.T. Jones and S. Raby, Nucl. Phys. **B222**, 11 (1983); M. Claudson, L.
Hall and I. Hinchliffe, Nucl. Phys. **B228**, 501 (1983).
- [26] J.A. Casas, A. Lleyda and C. Muñoz, Nucl. Phys. **B471** (1996) 3, hep-ph/9507294.
- [27] Particle Data Group, S. Eidelman et al, Phys. Lett. **B592**, 1 (2004).
- [28] J.R. Ellis, K.A. Olive, Y. Santoso and V.C. Spanos, Phys. Lett. **B588**, 7 (2004),
hep-ph/0312262; L. Roszkowski, R. Ruiz de Austri and K.-Y. Choi, JHEP **0508**, 080
(2005), hep-ph/0408227.

- [29] L. Covi, L. Roszkowski, R. Ruiz de Austri and M. Small, JHEP **0406**, 003 (2004), hep-ph/0402240.
- [30] For an up-to-date summary of sparticle search limits from the LEP experiments, see <http://lepsusy.web.cern.ch/lepsusy/> .
- [31] The ALEPH, DELPHI, L3 and OPAL Collab.s, Phys. Lett. **B565**, 61 (2003), hep-ex/0306033.
- [32] R. Barbieri and L. Maiani, Nucl. Phys. **B224**, 32 (1983); C.S. Lim, T. Inami and N. Sakai, Phys. Rev. **D29**, 1488 (1984); E. Eliasson, Phys. Lett. **147B**, 65 (1984); M. Drees and K. Hagiwara, Phys. Rev. **D42**, 1709 (1990).
- [33] A. Djouadi, P. Gambino, S. Heinemeyer, W. Hollik, C. Jünger and G. Weiglein, Phys. Rev. Lett. **78**, 3636 (1997), hep-ph/9612363, and Phys. Rev. **D57**, 4179 (1998), hep-ph/9710438.
- [34] S.P. Martin and J.D. Wells, Phys. Rev. **D64**, 035003 (2001), hep-ph/0103067.
- [35] G. Degrassi and G.F. Giudice, Phys. Rev. **D58**, 053007 (1998), hep-ph/9803384.
- [36] A.L. Kagan and M. Neubert, Eur. Phys. J. **C7**, 5 (1999); P. Gambino and U. Haisch, JHEP **0110**, 020 (2001), hep-ph/0109058, and JHEP **0009**, 001 (2000), hep-ph/0007259; P. Gambino, M. Gorbahn and U. Haisch, Nucl. Phys. **B673**, 238 (2003), hep-ph/0306079.
- [37] G. Degrassi, P. Gambino and G.F. Giudice, JHEP **0012**, 009 (2000), hep-ph/0009337.
- [38] K. Okumura and L. Roszkowski, Phys. Rev. Lett. **92**, 161801 (2004), hep-ph/0208101.
- [39] See e.g. F. Borzumati, C. Greub, T. Hurth and D. Wyler, Phys. Rev. **D62**, 075005 (2000), hep-ph/9911245, and references therein.
- [40] M. Drees, talk held at *SUSY2004*, Tsukuba, Japan, June 2004, hep-ph/0410113.
- [41] D0 Collab. V.M. Abazov et al., Nature **429**, 638 (2004), hep-ex/0406031.
- [42] L.S. Stark P. Hafliger, A. Biland and F. Pauss, JHEP **0508**, 059 (2005), hep-ph/0502197.

- [43] H. Baer, A. Belyaev, T. Krupovnickas and X. Tata, JHEP **0402**, 007 (2004), hep-ph/0311351; H. Baer, T. Krupovnickas and X. Tata, JHEP **0406**, 061 (2004), hep-ph/0405058; A. Djouadi, M. Drees and J.L. Kneur, Phys. Lett. **B624**, 60 (2005), hep-ph/0504090.
- [44] M. Drees and M.M. Nojiri, Phys. Rev. **D47**, 376 (1993); T. Falk, R. Madden, K.A. Olive and M. Srednicki, Phys. Lett. **B318**, 354 (1993), hep-ph/9308324.
- [45] C. Boehm, A. Djouadi and M. Drees, Phys. Rev. **D62**, 035012 (2000), hep-ph/9911496; R. Arnowitt, B. Dutta and Y. Santoso, Nucl. Phys. **B606**, 59 (2001); J.R. Ellis, K.A. Olive and Y. Santoso, Astropart. Phys. **18**, 395 (2003).
- [46] See e.g. M. Drees, R.M. Godbole and P. Roy, *Theory and Phenomenology of Sparticles*, World Scientific (Singapore, 2004).
- [47] U. Ellwanger, Phys. Lett. **B141**, 435 (1984).
- [48] For a recent review, see A. Djouadi, hep-ph/0503173.
- [49] M. Drees and M.M. Nojiri, Phys. Rev. **D45**, 2482 (1992).
- [50] K. Griest and M. Kamionkowski, Phys. Rev. Lett. **64**, 615 (1990).
- [51] S.P. Martin and M.T. Vaughn, Phys. Lett. **B318**, 331 (1993), hep-ph/9308222.
- [52] M. Drees and M.M. Nojiri, Phys. Rev. **D48**, 3483 (1993), hep-ph/9307208; A. Djouadi and M. Drees, Phys. Lett. **B484**, 183 (2000), hep-ph/0004205.
- [53] See e.g. J.R. Ellis, J.L. Feng, A. Ferstl, K.T. Matchev and K.A. Olive, Eur. Phys. J. **C24**, 311 (2002), astro-ph/0110225.
- [54] CDMS Collab., D.S. Akerib et al., astro-ph/0509259.
- [55] See e.g. H. Baer, C. Balazs, A. Belyaev, T. Krupovnickas and X. Tata, JHEP **0306**, 054 (2003), hep-ph/0304303.
- [56] See e.g. Tevatron Higgs Working Group Collab. M. Carena et al., hep-ph/0010338.